MASTER OF SCIENCE BY RESEARCH

An investigatory study into improving vehicle control by the use of direct real time slip angle sensing

Sriskantha, Jega

Award date:
2016

Awarding institution:
Coventry University

An Investigatory Study into Improving Vehicle Control by the use of Direct Real Time Slip Angle Sensing

By

Jega Sriskantha

February 2016

An Investigatory Study into Improving Vehicle Control by the use of Direct Real Time Slip Angle Sensing

By

Jega Sriskantha

February 2016

A thesis submitted in partial fulfilment of the University's requirements for the Degree of Master of Research

DECLARATION

A thesis submitted in partial fulfilment of the University's requirements for the Master of Research award.

This project is all my own work and has not been copied in part or in whole from any other source except where duly acknowledged. As such, all use of previously published work (from books, journals, magazines, internet, etc…) has been acknowledged within the main report to an item in the References or Bibliography lists.

I also agree that an electronic copy of this project may be stored and used for the purposes of plagiarism prevention and detection.

Copyright Acknowledgement

Signed: _____

Date: 18th May 2015

ACKNOWLEDGEMENTS

The author would like to show the utmost gratitude to the author's family and friends for their, support, guidance and forbearance with the author whilst the project was being completed.

ABSTRACT

The following document sets out to determine the key limitations to existing methods of acquiring body slip angle data and how could accurate live body slip angle provide better information about a vehicle's current behavior to aid vehicle safety systems.

Initially, body slip angle estimation techniques are evaluated as these methods are currently used in electronic stability control systems, as current vehicles do not have body slip angle sensors. It is clear to see that all the different estimations methods have clear limitations. With this in mind existing methods of measuring body slip angle were investigated, such as optical sensors, GPS and Doppler velocity sensors. It is clear that laser Doppler velocity sensors could be an accurate method of measuring body slip angle on consumer vehicles, therefore a body slip angle based electronic stability control system using laser doppler velocity sensors is proposed.

In order to further validate body slip angle based electronic stability control systems, several multi body simulations are carried out. The multi body simulations show that an electronic stability control system based on body slip angle is feasible. The simulations also show that in low coefficient of friction conditions the body slip angle is a better indicator of vehicle behavior than yaw rate.

In conclusion, it is clear to see that there is a need in the automotive industry for direct real time slip angle sensors, but further research is required to determine the robustness and viability of body slip angle targeted ESC systems.

Table of Contents

TABLE OF FIGURES

TABLE OF EQUATIONS

LIST OF TABLES

Nomenclature

$a = Distance\ From\ Front\ Axle\ to\ Centre\ of\ Gravity$

$\alpha_i = Tyre\ Slip\ Angle, Where\ Index\ i\ Indicates\ Front\ or\ Rear\ Axle$

$a_y = Lateral\ Acceleration$

$\alpha_f = Front\ Axle\ Slip\ Angle$

$\alpha_r = Rear\ Axle\ Slip\ Angle$

$a_{y\,max} = Maximum\ Lateral\ Acceleration$

$Ay_{meas} = Measured\ Vehicle\ Lateral\ Acceleration$

$A_y = Lateral\ Acceleration$

$A_z = Verticcal\ Acceleration$

$\alpha = Tyre\ Slip\ Angle$

$b = Distance\ From\ Rear\ Axle\ to\ Centre\ of\ Gravity$

$bf = Cut\ Off\ Frequency\ of\ a\ Low\ Pass\ Filter$

$\beta = Vehicle\ Body\ Slip\ Angle$

$\dot{\beta} = Body\ Slip\ Angle$

$\dot{\beta} = Body\ Slip\ Angle\ Rotational\ Velocity$

$\hat{\beta}_{kin} = Estimated\ Body\ Slip\ Angle\ from\ Kinematics\ Based\ Estimation$

$\hat{\beta}_m = Estimated\ Body\ Slip\ Angle\ using\ Model\ Based\ Estimation$

$c = Signal\ Wave\ Velocity$

$c_1 = Model\ Parameter$

$c_2 = Model\ Parameter$

$C_f = Front\ Tyre\ Conering\ Stiffness$

$C_r = \ Rear\ Tyre\ Cornering\ Stiffness$

$\delta = Steer\ Angle\ of\ Front\ Axle$

$\delta = Steering\ Wheel\ Angle$

$\delta_f = Front\ Wheel\ Steering\ Angle$

$f = Frequency$

$f_{source} = Frequency\ of\ Source\ Signal$

$F_f = Front\ Axle\ Lateral\ Force$

$F_r = Rear\ Axle\ Lateral\ Force$

$F_X = Longitudinal\ Force$

$F_y = Lateral\ Force$

$F_Y = Lateral\ Force$

$F_{yf} = Sum\ of\ Front\ Tyre\ Lateral\ Force$

$F_{yf} = Front\ Axle\ Lateral\ Force$

$F_{yf\ max} = Max\ lateral\ Force\ on\ Front\ Axle$

$F_{yi} = Lateral\ Force\ , Where\ Index\ i\ Indicates\ Front\ or\ Rear\ Axle$

$F_{yr} = Sum\ of\ Rear\ Tyre\ Lateral\ Force$

$F_{yr\ max} = Max\ Lateral\ Force\ on\ Rear\ Axle$

$F_{yr} = Rear\ Axle\ Lateral\ Force$

$Fz = Tyre\ Vertical\ Force$

$F_{zf} = Vertical\ Force\ on\ Front\ Axle$

$F_{zr} = Vertical\ Force\ on\ Rear\ Axle$

$g = Gravity$

$g = Acceleration\ Due\ to\ Gravity$

$J = Moment\ of\ Inertia\ Around\ the\ Vertical\ Axis\ Through\ the\ Centre\ of\ Gravity$

$K = Stability\ Factor$

$l = Wheelbase$

$l_f = Longitudinal\ Distance\ to\ the\ Centre\ of\ Gravity\ from\ the\ Front\ Axle$

$l_r = Longitudinal\ Distance\ to\ the\ Centre\ of\ Gravity\ from\ the\ Rear\ Axle$

$m = Vehicle\ Mass$

$m = Mass\ of\ Vehicle$

$M = Total\ Vehicle\ Mass$

$N_\beta = Static\ Directional\ Stability\ Derivative$

$N_\delta = Control\ Moment\ Derivative$

$\sigma_x = Longitudinal\ Slip\ Ratio$

$\Omega = Vehicle\ Yaw\ Rate$

$\phi = Vehicle\ Roll\ Angle$

$\phi r = Road\ Bank\ Angle$

$r = Yaw\ Rate$

$r_{meas} = Measured\ \ Yaw\ Rate$

$\tau = Time\ Constant$

$\mu = Road\ Surface\ Friction\ Coefficient$

$u = Vehicle's\ Longitudinal\ Velocity$

$\hat{\mu} = Road\ Surface\ Friction\ Coefficient$

$\mu_{ice} = Road\ Surface\ Friction\ Coefficient\ For\ Icy\ Road\ (\ Typically\ 0.1)$

$\mu_{dry} = Road\ Surface\ Friction\ Coefficient\ For\ Dry\ Road\ (\ Typically\ 1.0)$

$\mu_{f\ max} = Maximum\ Tyre - Road\ Friction\ Coefficient\ on\ Front\ Axle$

$\mu_{r\ max} = Maximum\ Tyre - Road\ Friction\ Coefficient\ on\ Rear\ Axle$

$v = Longitudinal\ Velocity$

$v = Velocity\ of\ Signal\ Receiver$

$V = Velocity$

$\dot{v}COG = Total\ Velocity\ at\ the\ Centre\ of\ Gravity$

$\dot{v}_y = Lateral\ Velocity\ at\ Centre\ of\ Gravity$

$\dot{v}_y = Lateral\ Velocity$

$v_x = Longitudinal\ Velocity$

$V_x = Longitudinal\ Velocity$

$\dot{v}_{ye} = Lateral\ Velocity\ Estimation$

$YRG = Yaw\ Rate\ Gain$

$Y_\beta = \ Damping\ in\ Side\ Slip\ Derivative$

$Y_\delta = Control\ Force\ Derivative$

$\dot{\psi} = Yaw\ Velocity$

$\dot{\psi} = Yaw\ Rate$

$\omega = Longitudinal\ Acceleration$

$\omega_z = Vehicle\ Yaw\ Rate$

$\Psi_{GPS}^{Vel} = \ Horizontal\ GPS\ Velocity\ Vector\ Heading$

$\Psi = Orientation\ of\ the\ Vehicle\ Centreline\ (Vehicle\ Heading)$

$\Psi_{GPS}^{Vel} = \ Horizontal\ GPS\ Velocity\ Vector\ Heading$

$\Psi = Orientation\ of\ the\ Vehicle\ Centreline\ (Vehicle\ Heading)$

1.0 INTRODUCTION

Vehicle control is a widely researched area of vehicle dynamics that has always been a staple area of enhancement during the development process of vehicles. A strong understanding of vehicle behaviour in regards to control is necessary, as a vehicle with poor control has dangerous safety implications. In order to improve vehicle control and safety, numerous intelligent safety systems have been implemented into vehicles, such as; Anti-lock Braking Systems (ABS), Electronic Stability Control (ESC) and torque vectoring.

Although some of these safety systems have significantly improved vehicle safety, such as ESC providing a 43% reduction in fatal crashes in the USA as seen in Figure 1, there is still a global demand to improve vehicle safety. Action plans such as the United Nation's (UN's) Decade of Action for Road Safety are encouraging the development, deployment and accelerated uptake of credible safety systems (Global NCAP, 2012-2013).

Figure 1 Studies on Electronic Safety Program (ESP) effectiveness in accident reduction [Liebemann E, 2007]

Vehicle safety systems such as ESC aim to improve vehicle control, specifically in regards to vehicle path, by measuring and controlling the body slip angle and the yaw rate of a vehicle. The body slip angle is the angle between the vehicles heading and the direction of its travel, this is also referred to as side-slip angle. The yaw rate is the vehicle's angular velocity about its yaw

axis. Simplistically an ESC system aims to control the body slip angle and yaw rate, by controlling the longitudinal brake torque at individual wheels. Fundamentally, the body slip angle and yaw rate are highly dependent on the dynamic behaviour of the tyres. The dynamic behaviour of a tyre is due to a variety of factors, such as the road tyre friction coefficient, tyre temperature and the tyre stiffness, for a given steered situation a common measure of the tyres ability is its slip angle. A tyre's slip angle is the angle between the tyre's heading and the tyre's direction of travel.

A key aspect of intelligent vehicle control systems such as ESC, is the estimation or the measuring of current vehicle states and the estimation of vehicle desired states. In the case of an ESC system the key states would be the vehicle's yaw angle and body slip angle. Current ESC systems use the components required for ABS systems (wheel-speed sensors, hydraulic modulation units and an electronic control unit) coupled with a steering wheel angle sensor, a yaw rate sensor, a lateral acceleration sensor and a brake pressure sensor to determine the vehicle's current state, desired state and control the vehicle with the aim to achieve the desired state (Zanten, 2000).

In recent years the research into vehicle control systems, and therefore vehicle state estimation has significantly increased due to the demand and interest of autonomous vehicles. The design and development of autonomous vehicle's pose complex control problems where the autonomous vehicle will not only need to have intelligent systems that have complete control of the vehicle, but have highly robust methods of state estimation in order to avoid continuous miscalculations due to sensor drift.

In 2003 DARPA (Defence Advanced Research Project Agency) introduced the DARPA Grand Challenge which was created with the goal to develop an autonomous robot capable of traveling through 142 miles of unrehearsed off road terrain. The first robot to successfully achieve this was Stanford University's "Stanley" a heavily sensor laden and computationally equipped Volkswagen Touareg (Thrun, et al., 2006). In comparison to production road vehicles Stanley's vehicle estimation requirements were significantly more complex. Stanley's complex vehicle state estimation required; three position state variables, three velocity state variables, three orientation state variables, three accelerometer bias state variables and three gyro bias state variables (Thrun, et al., 2006). All fifteen of these state variables would need to be measured or estimated. In order to successfully measure or estimate these states sensor technology typically not used for automotive control applications needed to be utilised as

traditional existing sensors would not suffice. Stanley used GPS, a GPS compass and an IMU (inertia measurement unit) in order to determine the vehicle state variables. The use and uptake of new technologies in the automotive industry, has been slow and typically required years of validation and homologation, but research in autonomous vehicles is encouraging a shift in the culture for the uptake of new technologies, as consumer vehicle requirements are changing quickly and with additional complexity. With this in mind, there is significant scope to use new technologies to bridge the gap between traditional vehicles and autonomous vehicles, these being traditional vehicles with advanced vehicle control systems.

As body slip angle is a key vehicle state for ESC systems, the use of new technology to directly measure the body slip angle in real time and implementing it into the ESC system could prove beneficial in improving vehicle control and safety, with this in mind the following investigation has been composed, with the aim to satisfy the following question;

What are the key limitations to existing methods of acquiring body slip angle data and how could accurate live body slip angle provide better information about a vehicle's current behavior to aid vehicle safety systems?

Existing literature on acquiring real time body slip angle data for the use in vehicle safety systems is limited, with the majority of literature on body slip angle measurement focusing on the accuracy of the technologies used, but not focusing on how this data could be successful used in vehicle safety systems. Existing literature is also limited on the robustness of traditional ESC systems (that use yaw rate sensors) for certain conditions such as on low friction road surfaces, with these limitations in mind and with the intent to satisfy the research question the following project aims have been determined;

- Determine the advantages of acquiring direct real time slip angle data on automobiles.
- Determine the suitability of various technologies in order to acquire real time slip angle data.
- Determine the limitations of existing hardware and software required for implementation of a live slip angle sensing system.
- Determine suitable areas of development that will create further benefit of slip angle data.

2.0 REAL TIME SLIP ANGLE SENSING

2.1 The Importance of Yaw Rate

Yaw is the rotation about the yaw axis, which is the rotation of the vehicle when seen in plan view. Simplistically if a vehicle yaws too little for a given handwheel input the vehicle can be considered as under-steering and if the vehicle yaws too much the vehicle can be considered as over-steering, this information can be beneficial in understanding a vehicle's current state.

The yaw rate (yaw velocity) is the rate of change of yaw with respect to time. In order to change the path of a vehicle, the driver applies a yaw rate demand at the handwheel; the demand for rotational velocity coupled with longitudinal acceleration generates lateral forces at the tyres in order to generate a yaw moment about the yaw axis of the vehicle, this yaw moment causes a change in the vehicle's heading.

At low vehicle speeds ~15 miles per hour (mph), the maximum achievable yaw rate is determined by the vehicle's geometry, above this speed, slip angle at the tyres combined with tyre-road surface friction have a significant effect on the yaw rate. When the vehicle is traveling at high speeds small yaw rate demands at the hand wheel can cause the available friction to saturate, causing loss of vehicle control (Blundell & Harty, 2004) .

The yaw rate will vary due to the steer angle and speed; yaw rate gain is commonly used to determine vehicle stability. The yaw rate gain is the yaw rate divided by the steered road wheel angle; typically yaw rate gain has a non-linear relationship with vehicle speed. The vehicle stability can be determined from the yaw rate gain (YRG) by understanding the stability factor metric K. Stability factor K can be determined by the following equations:

Equation 1 Stability Factor K (Milliken & Milliken, 1995)

Equation 2 Yaw Rate Gain in Terms of Stability Factor (Milliken & Milliken, 1995)

Equation 2 shows that when K is zero, the vehicle has neutral steer response, i.e. the yaw rate gain is only dependant on the vehicle velocity and wheelbase and therefore does not understeer or over steer. When K is not zero, the sign of K significantly affects the vehicle responses; when K is positive the vehicle's yaw rate gain (and therefore vehicle response) decreases as the vehicle speed increases and when K is negative the yaw rate gain increases with vehicle speed. This can be seen in Figure 2.

Figure 2 YRG vs Forward Velocity: Understanding the Significance of Stability Factor K (Milliken & Milliken, 1995)

When K is negative, the vehicle is over-steering and when K is positive, the vehicle is under-steering. As previously mentioned small yaw rate demands at high speed can cause the available tyre-road friction to saturate, therefore for typical road vehicles it is ideal to have K positive (the vehicle under-steering), this way the vehicle's sensitivity to yaw rate demands reduces as the vehicle speed increases. If K is negative this may lead to divergent instability at high vehicle speeds.

In summation the yaw rate of the vehicle has a significant effect on the stability of the vehicle and the yaw rate gain can provide invaluable information on the general dynamic characteristics of a vehicle.

Regardless of whether a vehicle has a positive or negative stability factor a lower yaw rate gain is desirable as the vehicle can still be controlled and the likelihood of saturation of the road tyre friction is low. Altering the yaw rate or the steered wheel angles can control the yaw rate gain; the complexity associated with controlling the steered wheels makes controlling the yaw rate ideal. Maintaining a low yaw rate during evasive manoeuvres will allow for greater control of a vehicle. Active vehicle safety systems such as ESC set out to control the yaw rate or achieve a desirable yaw rate gain.

The yaw rate of a vehicle can be determined by the use of a yaw rate sensor, which uses the Coriolis effect to determine the vehicle yaw rate. Yaw rate sensors are now common sensors found on many automotive vehicles.

2.2 Electronic Stability Control Systems

Electronic stability control (ESC) is a yaw stability control system that aims to prevent spin out (excessive oversteer) and plough (excessive understeer). The ESC systems aims to prevent spin out and plough by compensating the yaw moment on the vehicle. Figure 3 shows an example of how an ESC system can use brake force to control the vehicles path, and how a vehicle behaves with and without ESC.

Figure 3 How excessive over-steer (spin out) and excessive under-steer (plough) can be controlled in critical situations with the use of an ESC system (Lee, 2007)

When a vehicle is spinning out, the yaw rate on the vehicle is higher than expected and therefore the vehicle steers too much in relation to the desired path, this tends to occur when the vehicle is on its limits. Figure 3 (a) Spin out, clearly shows that in order to prevent spin out a braking force is applied to the front outside wheel. Applying a braking force can have two main effects; adjusting the yaw moment on the vehicle and adjusting the lateral forces at the wheel.

Simplistically applying a braking force on the front outside wheel, when the vehicle is spinning out, will create a corrective yaw moment, in the opposite direction of the existing yaw moment that is causing the vehicle to spin out, that will allow the vehicle to achieve its desired path. Braking the front outside wheel, will also reduce the lateral force at the tyre, this can be understood when plotting at the longitudinal force against lateral force as seen in Figure 4. It is clear to see when looking at Figure 4, that when braking force is increased the lateral force on the tyre reduces for a given slip angle. Reducing the lateral force, will also reduce the initial yaw moment, causing the vehicle to spin out.

Figure 4 Plotting Lateral force against Longitudinal Force [Friction Circle] (Blundell & Harty, 2004)

When the vehicle is ploughing, the yaw rate on the vehicle is lower than expected and the vehicle does not steer as enough to achieve the desired path. Braking the rear inside wheel as seen in Figure 3 (b) plough, corrects the yaw moment, by increasing the yaw moment in the direction of the existing yaw moment. As with the spin out scenario, braking the rear wheel, will also reduce the lateral force available at the rear tyre, which will reduce the forces opposing the yaw moment in the desired direction.

The three main technologies used in stability control systems to control a vehicle's yaw moment are, differential braking, steer-by-wire and torque vectoring (Rajamani, 2006).

- Differential braking is the system seen above, where braking forces are distributed to each wheel, typically by using a vehicle's ABS system.
- Steer by wire is where the steering input that is usually applied by the driver at the steering wheel is modified in order to achieve the desired yaw rate.
- Torque vectoring is similar to differential braking, but instead of braking, a torque is applied to the individual wheels, by the use of either active differentials or hub centred motors on electric vehicles.

All ESC systems tend to use the same principles, regardless of the technology that is utilised to achieve the desired yaw moment. ESC systems can be considered as reactive systems that are active once the vehicle is no longer at the desired yaw rate.

Continuing with the differential braking example, the control architecture of this type of ESC system can be seen in Figure 5. The ESC system utilises two controllers. The upper controller determines the desired yaw torque, based on wheel speed, lateral acceleration, yaw rate and steering angle measurements. The lower controller determines the brake pressure inputs to achieve the desired yaw rate from the upper controller.

Figure 5 An example structure of an Electronic Stability Control System (Rajamani, 2006)

The upper controller determines the desired yaw torque by the use of a sliding mode controller, if the sliding mode controller successfully converges to the surface so that s = 0, the desired yaw rate is obtained. The controller not only requires the wheel speed, lateral acceleration, yaw rate and steering angle measurements but also estimates body slip angle and front and rear tyre lateral force feedback. The body slip angle and tyre lateral forces are currently estimated as they are not easily measured (Rajamani, 2006).

The lower controller determines the required brake pressure inputs, based on the desired yaw torque determined by the upper controller. The controller determines initially what differential longitudinal tyre forces are required in order to achieve the desired yaw torque. The controller then determines what braking pressures are required to achieve the desired longitudinal forces. The controller requires driver throttle input, input from the traction control system and brake pressure measured at the wheel at the initiation of differential braking, in order to determine what brake pressures are required (Rajamani, 2006).

2.3 The Importance of Body Slip Angle

As with yaw rate, the body slip angle is generated due to the driver initiated yaw rate demand at the handwheel, this yaw rate demand creates a slip angle at the front tyres and as the lateral acceleration of the vehicle begins to increase the slip angle at the rear tyres is generated. The slip angle of the tyres is the angle between the tyre's direction of travel and the tyre's heading. The variation between the direction of travel at the front axle and the direction of travel at the rear axle generates a body slip angle. The body slip angle, is the angle between the vehicle's direction of travel and the vehicle's heading.

A vehicle's body slip angle is highly dependent on the tyre – road friction, low friction at the tyres (and therefore low adhesion) will lead to relatively high body slip angles when compared to high friction (and inherently high adhesion) at the tyres for a given yaw rate, this can be seen in Figure 6. It is because of this relationship between body-slip angle and road-tyre friction that body slip angle is commonly used as a measure of vehicle manoeuvrability or controllability.

Figure 6 The effect of road surface friction coefficient on vehicle path and how yaw stability control can contribute to vehicle path control (Rajamani, 2006)

Under typical driving conditions, it is unlikely that drivers will exceed body slip angles greater than ~2 degrees. This is not the case in accident situations, data based on a study of 17000 car accidents show that 20-25% of accidents were due to vehicles spinning and 60% of which involved a single car, this suggests that a significant proportion of accidents involve high-uncontrolled vehicle slip angles. This is somewhat expected because when the tyres reach their limits of adhesion and the body slip angle is high, the effect of yaw rate demands by the driver become significantly reduced (Zanten, 2000). Therefore, any handwheel demands initiated by the driver immediately prior to an accident would have minimal effect.

Typical drivers are unaware of the tyre adhesion limits of a vehicle, the adhesion limits of a vehicle are between ~10 -12 degrees on a dry asphalt road surface and between ~2-4 degrees on ice. If a vehicle approaches these adhesion limits vehicle control is effectively lost.

As a high slip angle suggests low manoeuvrability or controllability and therefore divergent vehicle behaviour, it is ideal to have controlled vehicle body slip angle so that it was consistently low (in order to maintain yaw moment gain) ; even during evasive manoeuvres, this is a task that vehicle safety systems such as ESC set out to achieve.

Unfortunately, unlike yaw rate sensors, body slip sensors are not part of the standard sensor setup commonly found on road vehicles. As real time body-slip angle is considered an important input into certain vehicle safety systems as it can be used as a measure of manoeuvrability or controllability it is commonly estimated. Due to high importance of real-time body slip angle, body slip angle estimation techniques are widely researched.

2.4 Estimating Body Slip Angle

As previously mentioned body slip angle is considered an important input into vehicle safety systems, but unlike yaw rate sensors, body slip sensors have not been implemented into the standard sensor set available in most vehicles, fundamentally because currently available sensors used in vehicle validation and homologation are expensive. In order to overcome this, several body slip angle estimation techniques have been proposed each with their own advantages and disadvantages.

2.4.1 Dynamic Model Based Estimators

Dynamic based estimators are the most commonly used method of body slip angle and lateral velocity estimation. This type of estimation fundamentally uses handling models and state space observers. Many variations of dynamic model based estimators have been investigated; the variations in these estimators include variations in both the underlying dynamic model and the state space observer.

The accuracy of body slip angle estimation from the state observers is directly related to the accuracy of the underlying dynamic model. It is because of this that various researchers have proposed different models and observers. Shraim et al., (Shraim, et al., 2007), Hiemer et al., (Hiemer, et al., 2005) propose double track models as the underlying dynamic model, whereas Hac and Bedner (Hac & Bedner, 2007) proposes a single-track model (bicycle model).

Shraim et al., and Hiemer et al., use non-linear double track models based on fundamental dynamic principles; both Shraim et al., and Hiemer highlight that their models fundamentally calculate vehicle velocity ($\dot{v}$) and Body slip angle ($\dot{\beta}$) by the use of Equation 3 and Figure 4 respectively.

Equation 3 Non-Linear Double Track Acceleration at COG

.

Equation 4 Non-Linear Double Track Beta Dot

Variations in the models occur in the calculation of the yaw moment about the centre of gravity (see Table 1) this is fundamentally due to the system inputs such as trail and gauge.

Table 1 Non-Linear Double Track Model Comparison

The main differences occur in these models at the lateral and longitudinal force estimation, which provides the non-linearity in the model. The complexity in tyre behaviour that leads to the model linearity is the main reason why robust body slip angle estimators are so widely researched.

Shraim et al., uses a 3rd order sliding mode observer to determine the wheel angular velocities and longitudinal force. Shraim et al., then uses another super twisting algorithm based sliding mode observer to determine the side slip angle and velocity and then uses this information to calculate the longitudinal velocity, lateral velocity and lateral forces. This method when compared to simulation results showed good correlation with motor torque, braking torque, angular position, angular velocity, steering angle, and vehicle velocity and slip angle. On the other hand Hiemer et al., use measured wheel loads, calculated tyre slip angles and a non-linear least squares technique to determine cornering stiffness at the axles and then modifies Equation 3, Figure 4 and Equation 6 Non-Linear Double Track Model Hiemer Moment Calculation (Hiemer, et al., 2005) to create new differential equations used for the state space model. Hiemer et al., then propose two observer strategies: a linearization observer and an AQF (Adaption of a Quality Function) observer (which required restructuring of the state space model), both of which again successfully show good body slip angle correlation when compared to real vehicle data.

Figure 7 Estimated Side Slip Angle (rad) using Sliding Mode Controller and that of a VE-DYNA [Real Time Vehicle Dynamics Software] Simulator (Shraim, et al., 2007)

Figure 8 Comparisons of Linearization Observer and AQF (Adaption of a Quality Function) Observer against measured data (Hiemer, et al., 2005)

When comparing the results seen in Figure 7 and Figure 8 it is clear that the observers are successful in estimating the body slip angle, with the sliding mode observer seen in Figure 7 having a maximum variation of ~0.0005 rad and both the linearization observer and AQF observer having a maximum of ~ 1 grad which is ~ 0.015 rad. It is interesting to note that although the sliding mode observer is the most accurate it takes the longest to converge. It is also worth mentioning that this comparison is far from ideal due to the variation in test conditions and the true ability of these observers cannot be directly compared.

Although both techniques have been able to accurately determine body slip angle, each of the techniques have limitations. A key limitation is that the estimation is only as accurate, as the underlying model is accurate to the physical vehicle. I.e. if the model is not representative of the vehicle, the body slip angle estimate will also not be representative of the vehicle. Furthermore, Heimer's underlying double track model requires tyre vertical loads, which is not a standard output from the sensor sets on current vehicles; therefore a robust feasibility study would be required in order to determine how tyre vertical load could be accurately determined before this technique can be implemented. Finally, the overall robustness of the estimators have not been determined in regards to their ability to determine body slip angle for a variety of situations such as low coefficient of friction, surfaces. With this in mind Hac & Bedner (Hac & Bedner, 2007) carry out a robustness investigation, on "a reduced order observer based on a

non-linear bicycle model and empirically determine tire lateral force characteristics" (Hac & Bedner, 2007) which takes tyre road surface friction into consideration.

Hac & Bedner's model is fundamentally based on Equation 9, which can be derived from the basic lateral force equation seen in Equation 7 and the kinematic relationship seen in Equation 8.

Equation 7 Lateral Force based on Simple Dynamics (Hac & Bedner, 2007)

Equation 8 Lateral Kinematic Relationship (Hac & Bedner, 2007)

Equation 9 Bicycle Model (Hac & Bedner, 2007)

Hac & Bedner state that;

"When a vehicle is near or at the limit of adhesion, tire forces and consequently yaw dynamics, depend strongly on the surface coefficient of friction"

(Hac & Bedner, 2007)

Considering this, Hac & Bedner introduce non-linearity based on the surface coefficient of friction into Equation 9 in the form of the front and rear lateral force estimation. The front and rear lateral forces are calculated using Equation 13 based on empirical lateral force vs. tyre slip angle lookup tables gathered for ice ($\mu = 0.1$) and dry ($\mu = 1$) surface coefficients of adhesion. The slip angles and μ are estimated based on Equation 10, Equation 11 and Equation

12 respectively. It is necessary to note that the values for $\hat{v}_y$ and $\hat{v}_x$,that are used for the tyre slip angle estimations are determined using the estimated value from the previous iteration.

Equation 10 Front Slip Angle Estimation (Hac & Bedner, 2007)

This item has been removed due to 3rd party copyright. The unabridged version of the thesis can be viewed in the Lanchester Library Coventry University.

Equation 11 Rear Slip Angle Estimation (Hac & Bedner, 2007)

This item has been removed due to 3rd party copyright. The unabridged version of the thesis can be viewed in the Lanchester Library Coventry University.

Equation 12 Surface Coefficient of Adhesion Estimation (Hac & Bedner, 2007)

This item has been removed due to 3rd party copyright. The unabridged version of the thesis can be viewed in the Lanchester Library Coventry University.

^

Equation 13 Lateral Force Estimation (Hac & Bedner, 2007)

This item has been removed due to 3rd party copyright. The unabridged version of the thesis can be viewed in the Lanchester Library Coventry University.

Initial test results from physical vehicle testing show that the body slip angle estimator can successfully estimate body slip angle on low mu surfaces as seen in Figure 9 but in order to determine the robustness of the body slip angle estimation technique Hac & Bedner carried out an investigation by simulation of a vehicle model in CarSim. The CarSim model is correlated to real vehicle test data, which was generated, from a variety of manoeuvres on dry asphalt, snow and ice.

The robustness investigation was carried out on dry asphalt, snow and ice with the following steering patterns; ramp steer, step steer, open loop lane change, slalom and fishhook, at the following initial speeds; 30,50,70,120,140 and 180 kph. The amplitudes, rates of change, and frequencies varied depending on the road surface and some tests were eliminated if the vehicle would remain in the linear range (Hac & Bedner, 2007). The investigation yields a list of factors and their overall effect on body slip angle estimation and their effect in regards to over- or under- estimation of body slip angle; this can be seen in Figure 10 and Table 2 respectively.

Figure 9 Physical Test Data acquired using optical sensors Vs. Dynamic Model based Estimation for a Lane Change Manoeuvre on Snow at 60 kph (Hac & Bedner, 2007)

This item has been removed due to 3rd party copyright. The unabridged version of the thesis can be viewed in the Lanchester Library Coventry University.

Figure 10 Average Maximum Increases in Estimation Errors due to Individual Factors, Where the Effect of A 10 Degree Bank Angle Corresponds to 1 (Hac & Bedner, 2007)

Table 2 Single Factors Contributing to Over - and Under- Estimation of Side Slip (Hac & Bedner, 2007)

This item has been removed due to 3rd party copyright. The unabridged version of the thesis can be viewed in the Lanchester Library Coventry University.

It is clear to see from the results that the accuracy of body slip angle estimation varies the most due to bank angle, as this seems to have a significant effect on the measured lateral acceleration. The data suggests that as the magnitude of bank angle increases the error in body slip angle estimation increases, the data also suggests that the bank angle direction directly effects whether the body slip angle is under or over estimated. Overall the results show that the accuracy of body slip angle is affected by discrepancies in the underlying dynamic model. For example, the underlying model does not take road bank angle into consideration as seen in Equation 9, which is why bank angle had such a significant effect on the body slip angle estimation.

Although this estimation technique has been proven to yield relatively accurate body slip angle estimations, and a strong understanding of the potential sources of error and their magnitude are made clear, the underlying model requires lateral force vs. slip angle lookup tables at high and low road surface adhesion coefficients. Acquiring this data for a vehicle is difficult and the data acquired will be specific to a certain vehicle and tyre setup and as Table 2 shows an estimation error of 0.2 (which is 20% of the error seen when there is a 10-degree bank angle) can be made from the tyre parameters alone. Therefore, this estimation technique cannot be easily and cost effectively adapted for multiple vehicles.

In summation body slip angle can be estimated successfully by the use of either double track or single-track dynamic models, but the accuracy of estimation is fundamentally dependant on sensor errors and on the underlying model based on specific parameters, which occasionally require either additional sensors or empirical data. It is worth noting that the robustness data from Hac & Bedner only determines the effect of single factors on body slip angle estimation, an understanding of how combined multiple factors affect body slip angle have not been investigated, this could be a suitable area for further research, but it can be assumed that multiple factors will increase the error.

2.4.2 Kinematic Relationship based Pseudo-Integrator Estimators

Kinematic pseudo-integrator based estimators are another commonly used type of body slip angle estimation. These types of estimators fundamentally use kinematic relationships to determine the body slip angle. Similar to the single-track model detailed above, kinematic estimators;

"Have not been [successful] in production vehicles primarily because of insufficient robustness on banked roads due, to inability to discriminate between the effect of change in lateral velocity and the effect of bank angle on measured lateral acceleration"

(Hac, et al., 2010)

In order to overcome the insufficient robustness Hac et al., propose both a roll angle estimator and a body slip angle estimator, in order to combine sensor information from multiple vehicle safety systems (ESC and occupant protection) to increase the robustness of both estimations. Hac et al., proposes to use the roll angle estimation to remove the gravity component of the lateral acceleration, which is due to the road bank angle.

As previously emphasised, the road bank angle can have a significant effect on the lateral velocity estimation and therefore the body slip angle estimation. The kinematic relationship of lateral acceleration can be adapted to take the effect of gravity, due to bank angle, into consideration. The modified kinematic relationship with the inclusion of bank angle can be seen in Equation 14. Unfortunately, pure integration of lateral acceleration based on Equation 14, to determine lateral velocity is infinitely sensitive to constant sensor errors, such as sensor bias and slow drifts. With this in mind Hac et al., propose a pseudo integration estimation method "which is essentially low pass filtering" (Hac, et al., 2010) this can be seen in Equation 15.

Kinematic pseudo integrator based estimators are significantly simpler than model based estimators, as the majority of the inputs required can be measured with the standard vehicle sensor set. The only input that requires calculation is the vehicle roll angle ϕ and as mentioned above, Hac et al. propose a kinematic pseudo integrator to estimate the vehicle roll angle using the roll rate sensor data.

Equation 14 Lateral Velocity from Kinematic Relationships (Hac, et al., 2010)

Equation 15 Pseudo Integration of Lateral Velocity Estimation based on Kinematic Relationships (Hac, et al., 2010)

A high value cut off frequency is beneficial for removing constant errors such as sensor bias, but can cause distortion because genuine low frequency components from the integrated signal are mitigated, this can be seen in Figure 11. Figure 11 shows lateral velocity estimates from a double lane manoeuvre, it is clear to see that the higher cut-off frequency yields more accurate results when there is a lateral acceleration bias, but lower accuracy when there is no lateral acceleration bias when compared to a lower cut of frequency. Hac et al., propose that by using either centring algorithms to remove sensor bias, or dynamically changing the cut of frequency dependant on the current vehicle conditions this compromise can be overcome (Hac, et al., 2010)

Figure 11 Estimate of Lateral Velocity in a Double Lane Change Manoeuvre with Different Filter Parameters (Hac, et al., 2010)

The Kinematic pseudo-integrator based estimator is shown to successfully estimate body slip angle by using roll angle estimations to determine the gravity component of the lateral acceleration this can be seen in Figure 12. Figure 1Figure 13 shows the relatively accurate estimation of roll angle, lateral velocity and sideslip angle. It is interesting to note that lateral velocity estimation seems significantly more accurate than both the roll angle and the body slip angle, it can be therefore inferred that the inaccuracies of the body slip angle estimation may be due to the inaccuracies of the roll angle.

It is interesting to note the robustness of this estimation technique, even though there is a significant amount of difficulty in estimating longitudinal speed on low tyre road adhesion surfaces this estimation technique seems to relatively successful estimate roll angle, lateral velocity and body slip angle, this can be seen in Figure 12.

Figure 12 Estimated Roll Angle, Lateral Velocity and Side Slip Angle by the use of a Kinematic Pseudo Integrator (dashed) and Measured (solid) Signals in a Slide Manoeuvre on Slippery Surface (Hac, et al., 2010)

This item has been removed due to 3rd party copyright. The unabridged version of the thesis can be viewed in the Lanchester Library Coventry University.

Figure 13 Estimated Roll Angle, Lateral Velocity and Side Slip Angle by the use of a Kinematic Pseudo Integrator (dashed) and Measured (solid) Signals in a Fishhook Manoeuvre (Hac, et al., 2010)

Although the results show that the kinematic pseudo integration estimation technique can successfully and robustly estimate body slip angle, a key limitation of this technique is the compromise that may be required for the cut-off frequency statement in Equation 15. The cut off frequency, which designed to reduce sensor errors such as sensor bias, is still not completely robust. Hac et al., have proposed solutions to overcome this robustness but they have not been verified and therefore the compromise remains which means this technique is still potentially sensitive to sensor biases.

It is interesting to note that this simpler estimation process, when compared to the dynamic model based estimators, is relatively as robust and accurate and only requires inputs that are available from the standard vehicle sensor set. The proposed technique is intriguing, as unlike the previously mentioned techniques, this technique aims to, and successfully utilises measured and estimated signals from multiple sub systems, specifically the Electronic Stability Control System and the occupant protection system, in order to robustly estimate body slip angle.

Overall its clear to see that body slip angle estimators based on dynamic models and kinematic relationship are successful in estimating body slip angle, but it's clear to see that both methods have significant limitations. With this in mind Piyabongkarn et al (Piyabongkarn, et al., 2009), propose a body slip angle estimation technique that utilises both dynamic models and kinematic relationships.

2.4.3 Combined Dynamic Model and Kinematic Relationship Estimators

Piyabongkarn et al., (Piyabongkarn, et al., 2009) propose an estimator that utilises a dynamic model based body slip estimator and a kinematic relationship based body slip estimator, in the hope that limitations from both techniques can be minimised. As mentioned above dynamic model based estimators is limited to the accuracy of the underlying models, but unlike kinematic model based estimators, dynamic model based estimators are robust against sensor errors and road bank angle, as they do not involve the (direct or pseudo) integration of sensors. The kinematic relationship based estimators are beneficial because they do not require and underlying model and therefore are robust against discrepancies in vehicle data. Piyabongkarn et al., propose a closed loop observer technique that uses feedback in the form of error, which is determined as the differences between the measured signals, and the model-estimated signals. I.e. the difference between the kinematic relationship estimator and the dynamic model based estimator.

Equation 16 Dynamic Model Side Slip Angle Estimation (Piyabongkarn, et al., 2009)

Piyabongkarn et al, derive Equation 16 from a dynamic model to determine the body slip angle based on the following assumptions;

- *Lateral tyre force is proportional to slip angle*
- *A small steering angle is assumed*
- *The slip angles at the front and rear tires can be related to the body slip angle and yaw rate using linear approximations*
- *The effect of vehicle roll is neglected*
- *The effect of vehicle longitudinal forces is neglected*

(Piyabongkarn, et al., 2009)

A key parameter for Equation 16 is tyre-cornering stiffness. The tyre cornering stiffness is used in this equation to introduce the non-linearity of the lateral forces, which is required in order to make the model representative of a real vehicle. The tyre cornering stiffness is highly dependent on the tyre vertical force and the tyre road surface adhesion and typically exhibits non-linear behaviour as seen in Figure 14. Piyabongkarn et al., propose a method of cornering stiffness estimation based on the relationship between cornering stiffness and μF_z. Figure 15 shows that cornering stiffness varies with μF_z, and based on Figure 14 we can infer that the cornering stiffness varies linearly at lower slip angles.

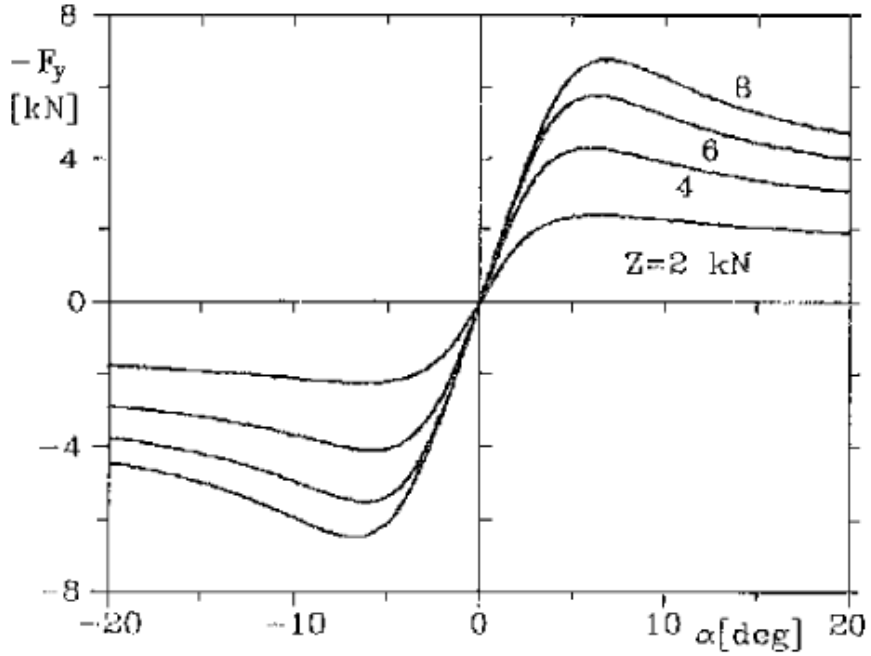

Figure 14 Lateral Tyre Force as a Function of Slip Angle at Various Values of μF_z

This item has been removed due to 3rd party copyright. The unabridged version of the thesis can be viewed in the Lanchester Library Coventry University.

Figure 15 Cornering Stiffness as Function of $_z$ (Piyabongkarn, et al., 2009)

In order to determine the cornering stiffness, Piyabongkarn et al. propose an estimation method for μF_z, so that cornering stiffness can be determined via the use of a lookup table with empirically gathered data such as that seen in Figure 15. As with the dynamic model proposed by Hac & Bedner (Hac & Bedner, 2007) empirical data is required to accurately determine the non-linearity of the vehicle.

Simplistically the μF_z is estimated by initially calculating the longitudinal slip ratio using Equation 17 to determine which model should be used to determine μF_z based on the normalised longitudinal tyre force plot seen in Figure 15. The cornering stiffness terms are then fed into Equation 16 to determine the body slip angle.

Equation 17 Longitudinal Slip Ratio Calculation (Piyabongkarn, et al., 2009)

This item has been removed due to 3rd party copyright. The unabridged version of the thesis can be viewed in the Lanchester Library Coventry University.

This item has been removed due to 3rd party copyright. The unabridged version of the thesis can be viewed in the Lanchester Library Coventry University.

Figure 16 Model of Normalised Longitudinal Force Vs. Slip Ratio for Friction Estimation Algorithm (Piyabongkarn, et al., 2009)

Piyabongkarn et al, then propose the use of Equation 18, which uses the kinematic relationships to determine the body slip angle. As previously mentioned this method is robust against variations in vehicle parameters, unlike Equation 16, as it does not require vehicle parameters such as cornering stiffness and vehicle mass. Similar to Equation 16, Equation 18 requires the additional estimation of another parameter in this case it is road bank angle. The road bank angle is estimated using a lateral accelerometer and an additional vertical accelerometer to determine A_{hoz} as seen in Figure 17. It is worth noting the accelerometers experience a net angle equal to bank angle – roll angle, due to the accelerometers being placed on the sprung mass (Piyabongkarn, et al., 2009) The value of A_{hoz} (horizontal acceleration) is determined by Equation 19, and used in Equation 20 to determine the road bank angle.

Equation 18 Kinematic Relationship Based Estimator (Piyabongkarn, et al., 2009)

This item has been removed due to 3rd party copyright. The unabridged version of the thesis can be viewed in the Lanchester Library Coventry University.

This item has been removed due to 3rd party copyright. The unabridged version of the thesis can be viewed in the Lanchester Library Coventry University.

Figure 17 The Estimation of Horizontal Acceleration Using Two Accelerometers For The Estimation of Road Bank Angle (Piyabongkarn, et al., 2009)

Equation 19 Horizontal Acceleration Calculation (Piyabongkarn, et al., 2009)

This item has been removed due to 3rd party copyright. The unabridged version of the thesis can be viewed in the Lanchester Library Coventry University.

Equation 20 Road Bank Angle Estimation (Piyabongkarn, et al., 2009)

This item has been removed due to 3rd party copyright. The unabridged version of the thesis can be viewed in the Lanchester Library Coventry University.

It is interesting to note than unlike Hac et al (Hac, et al., 2010) Piyabongkarn requires an additional sensor to determine the road bank angle, where Hac et al., use the existing sensors used in other subsystems.

With both dynamic and kinematic based estimators determined, Piyabongkarn et al., proposes a combined estimator that uses a first order filter as seen in Equation 21.

Equation 21 Combined Model and Kinematics Based Body Slip Angle Estimation [Piyabongkarn et al., 2009]

This item has been removed due to 3rd party copyright. The unabridged version of the thesis can be viewed in the Lanchester Library Coventry University.

With the use of the combined method it is clear to see that for both high and low friction surfaces the model is relatively accurate in estimation body slip angle, this can be seen in Figure 18 and Figure 19 It is interesting to note when looking at both figures that there are significant errors seen in both estimation methods, but these errors are successfully compensated for by the use of the combined method.

When comparing Figure 18(a) and Figure 19(a) it is interesting to see that the dynamic model based estimator significantly loses accuracy with the low friction road surfaces, this further emphasises the limitations stated previously. It is also interesting to see when comparing Figure 18(b) and Figure 19(b) that there does not seem to be a significant change in accuracy due to a change in road friction, again further emphasising the points previously mentioned. Figure 18(b) and Figure 19(b) also seem to have similar discrepancies between measured data as seen in Figure 11 where the sensor bias was having a significant effect on the estimation, therefore it can be inferred that sensor biases are also having a significant effect in Figure 18(b) and Figure 19(b).

Although the combined estimator aims to compensate for the limitations of the individual techniques the overall maximum, error increases from 0.435 degrees on the high μ road surface to 1.960 degrees on the low μ surface. As stated above this error seems to be carried forward from the dynamic model based estimation technique. Overall, the combined method seems to compensate for the errors in each of the individual methods due to their limitations, but their limitations are still carried forward to some extent in the combined model.

It is worth noting that the individual modelling techniques proposed by Piyabongkarn et al, seem to have significantly larger errors than the same techniques proposed by Hiemer et al (Hiemer, et al., 2005), Hac & Bedner (Hac & Bedner, 2007) and Hac et al (Hac, et al., 2010). Therefore, there could be some scope to increase body slip angle estimation accuracy by combining the techniques from the aforementioned authors. Limitations in Piyabongkarn et al., techniques could also be improved such as the using existing sensors as proposed by Hac et al, to determine road bank angle. The combined estimation technique is successful as it aims to reduce the limitations of the estimations techniques; another technique that aims to do this is Kalman Filter based estimators.

Figure 18 Slip Angle Estimation Results in Double Lane- Change test on High Friction Surface. (a) Model Based Method. (b) Kinematics Based Method. (c)Combined Method. (Piyabongkarn, et al., 2009)

Figure 19 Slip Angle Estimation Results in Double Lane-Change test on Low Friction Surface. (a) Model Based Method. (b) Kinematics Based Method. (c) Combined Method. (Piyabongkarn, et al., 2009)

2.4.4 Kalman Filter Body Slip Angle Estimator

Another commonly used estimation technique is via the use of a Kalman Filter, this technique is fundamentally a state space estimation (observer based) technique, which requires an underlying state space model which may be based on a dynamic model similar to the models mentioned previously. Kalman filters are linear quadratic estimators that are optimised to utilise inaccurate data to determine the current state of system providing that it is at least approximately linear and has Gaussian errors, therefore they are inherently beneficial for the use of body slip angle estimation.

Gao & Yu (Gao & Yu, 2010) propose the use of a discrete extended Kalman Filter (DEKF) based on a non-linear single-track model to determine body slip angle, like the use of the combined model, it is expected that the limitations from the underlying model will be carried forward, but the Kalman filter should appropriately compensate for these limitations. The proposed non-linear single model is fundamentally based on Equation 22.

Equation 22 Non-Linear Single Track Model (Gao & Yu, 2010)

As with the previous dynamic models, the variation in modelling technique arises with the modelling of the non-linearity of tyre behaviour and road surface friction, with this in mind Gao & Yu, propose the use of a non-linear tyre model based on Equation 23. The accuracy of the

data used for the tyre model will determine the accuracy of the model, Gao & Yu use a least squares technique to determine the tyre model parameters, front and rear tyre slip angle and front and rear lateral force, this can be seen in Equation 24, Equation 24,Equation 25, and Equation 26 respectively.

The accuracy of this model is then compared to both physically measured data and results from the use of a magic formula tyre model. It is clear to see from the results seen in Figure 20, that the proposed non-linear tyre model is representative of a real tyre, with the larger discrepancies only occurring at higher slip angles (above 3 degrees)

Equation 23 Arctangent Function for Non-Linear Relationship between Tyre Slip Angle and Tyre Lateral Force (Gao & Yu, 2010)

Equation 24 Front Slip Angle (Gao & Yu, 2010)

Equation 25 Rear Slip Angle (Gao & Yu, 2010)

This item has been

Equation 26 Front Lateral Force (Gao & Yu, 2010)

Equation 27 Rear Lateral Force (Gao & Yu, 2010)

Figure 20 Front and Rear Axle Comparisons of measured, ATAN model derived and magic formula derived lateral force vs side slip angle (Gao & Yu, 2010)

Based on the success of the results above, Gao & Yu then propose a non-linear model based on Equation 27 that also includes a road surface friction parameter. This can be seen in Equation 28. Gao & Yu then use μ_{max} (the maximum road-tyre friction coefficient) as a third state variable to create a state space model, to be observed by the discrete extended Kalman filter. The Kalman Filter is designed so that body slip angle, yaw rate and μ are observable states.

Equation 28 Non-Linear Tyre Mode with Friction Parameter (Gao & Yu, 2010)

Overall, the Kalman filter method is successful in estimation the body slip angle as seen in Figure 21. Figure 21 show the results from a sine steer test with increasing amplitude. It is interesting to note that the model alone (even with the inclusion of road surface friction estimation), without the Kalman filter is significantly less accurate; therefore, it can be assumed that the Kalman filter is successful in using the imprecise data to estimate the body slip angle. The Kalman filter technique also seems relatively accurate in the estimation of surface road friction; this can be seen in Figure 21. Figure 21 shows the results from a simulation carried out using CarMaker (a virtual test-driving platform simulation tool). The test consisted of varying the road surface from dry asphalt to an icy road to dry asphalt again. It is clear to see that Kalman filter takes a significant time to converge with the shortest time being ~10 seconds, although this method yields accurate body slip angle, using the tyre road friction information for other purposes may not be sufficient as the vehicle state could change dramatically with the 10 second convergence time. Finally, a key limitation to this method is lack of consideration to road bank angle, as many of the previous techniques have accounted for; although this technique is successful, its robustness against road bank angle has not been validated. Kalman Filters are widely considered successful in filtering out imprecise data, with that in mind they are used for a variety of purposes, Bevly et al., (Bevly, et al., 2006) propose the use of a Kalman Filter to combine GPS measurements and yaw gyroscope measurements as a technique to determine body slip angle.

Figure 21 Comparison of Side Slip Angle determined by CarMaker, Discrete Adaptive Extended Kalman Filter and Dynamic Model [Gao & Yu, 2010]

Figure 22 Discrete Extended Kalman Filter, Friction Coefficient Estimation (Gao & Yu, 2010)

Table 3 summaries the advantages and disadvantages, of the various body slip angle estimators researched, overall the body slip angle estimators can sufficiently estimate body slip angle, but they all have specific limitations based on their estimation technique. The majority of estimators researched are either dynamic model based or kinematic relationship based.

Although the dynamic model based estimators researched vary in both the underlying model and their observer strategy, there is a consistent limitation, this limitation is the relationship between the accuracy the body slip angle estimation and the accuracy of the underlying model. It is clear from the techniques researched that the difficulty arises in determining lateral force at the tyres as this commonly exhibits non-linear behaviour due to tyre road surface coefficient and tyre vertical load. Piyabongkarn et al, (Piyabongkarn, et al., 2009) and Hac & Bedner (Hac & Bedner, 2007) aim to overcome this issue by the use of empirical data. A key issue with using a dynamic model and empirical data is that both are specific to a vehicle and its setup and parameters, any variations in the setup or parameters could lead to inaccuracies in the estimated body slip. The fidelity of the underlying models also has a significant effect on the body slip angle estimation; an example can be seen in the models that do not incorporate road bank angle, Hac & Bedner, (Hac & Bedner, 2007) show that as the road bank angle increases the accuracy of body slip angle decreases. Simplistically these limitations can be overcome by directly measuring body slip angle or measuring tyre slip angle, as a direct measurement does not require specific vehicle parameters or an estimation of the vehicle non-linearity.

The kinematic relationship based estimators also vary in their techniques, but they also have a consistent limitation, this limitation is sensor error, specifically due to biases. Although the dynamic model based estimators also use the vehicle sensors, they do not involve the direct or pseudo integration of the sensors so the errors are not consistent as they are with the integration of the kinematic relationships. As with the dynamic model based estimators, the techniques try to reduce this limitation via the use of Kalman filtering or combining the kinematic integration technique with a dynamic model. Although these techniques are successful, the filtering required to remove the biases may also affect accurate data; therefore, a compromise in the accuracy of the body slip angle estimation will have to be made as highlighted by Hac et al., (Hac, et al., 2010). Again these limitations can be overcome by directly measuring body slip angle, although body slip angle sensors may also exhibit biases, they are

unlikely to require integration to determine body slip angle and will therefore be inherently less prone to the sensor biases.

In summation, the research shows a need for direct real time slip angle sensing, as current estimation techniques have limitations, are prone to errors and of en require specific vehicle parameters. With this in mind a method of real time slip angle sensing has been investigated.

Table 3 Advantages and Disadvantages of Body Slip Angle Estimators

Estimation Method	Advantages	Disadvantages
Dynamic Model Based Estimators	• Not significantly effected by sensor errors (such as bias) • A well correlated underlying model can produce accurate body slip angle results	• Typically require empirical data • May require additional sensors • Accuracy of results is directly related to non linear lateral force estimation • Requires accurate vehicle parameters
Kinematic Model Based Estimators	• Does not require accurate vehicle parameters • Relatively not sensitive to tyre road friction coefficient • Can produce accurate body slip angle results if road bank angle is considered	• Prone to inaccuracies from sensor errors • Compromise in body slip angle accuracy may be required in order to remove sensor biases • May require additional sensors to estimate road bank angle
Combined Kinematic and Dynamic Based Estimators	• Can significantly compensate for both model and sensor limitations such as sensor errors and model discrepancies	• Requires accurate vehicle parameters • Errors in underlying model for model based estimator, although compensated for are carried forward to overall estimation • May require empirical data • May require additional sensors
Kalman Filter	• Significantly compensates for errors in dynamic model • Not significantly affected by sensor errors (such as biases)	• Requires vehicle parameters • Tyre road friction coefficient estimation has long convergence time • May require additional sensors for road bank angle robustness

2.5 Real-Time Slip Angle Sensing

Real time slip angle sensors must be able to detect slip angle, as opposed to estimating slip angle, based on dynamic models or kinematic relationships. It is worth noting that kinematic estimators should not be considered as real time sensing, even though they fundamentally involve the integration of sensors. This is because they involve sensor integration based on an understanding of the kinematic relationships of a vehicle, to determine slip angle. There are two main techniques currently used for slip angle sensing these involve the use of Global Positioning Satellites (GPS) combined with Inertial Navigation Systems (INS), and optical velocity sensors. Both INS/GPS units and Optical velocity sensors are widely used in the automotive industry to measure body slip angle during vehicle testing and homologation, but fundamentally, both of these techniques have not been adopted in commercial vehicles due to their cost. As an alternative, the author proposes the use of Doppler velocity sensors, which are yet to be considered in the automotive industry for body slip angle estimation.

2.5.1 Real Time Body Slip Angle Sensing using GPS

An increasingly common technique of body slip angle sensing is via the use of INS/GPS units, Bevly et al., (Bevly, et al., 2006) and Beiker et al., (Beiker, et al., 2006) both propose the use of GPS for body slip angle sensing. Bevly et al., proposes two techniques of determining body slip angle by the use of GPS; the first technique involving a single GPS antenna and the second involving two GPS antennas, whereas Beiker et al., only proposes a technique that uses two GPS antennas.

GPS can be used to determine both position and velocity. Position can be determined via the use of multiple satellites (typically a minimum of four are required) (Beiker, et al., 2006). As the satellites position at a given time are known, the distance between the receiver and the satellites can be determined, these distances and the use of simple triangulation can determine the position of the receiver. The velocity of the receiver is determined using the Doppler Effect, the Doppler Effect is the change in frequency of a wave signal due to the relative motion between a source and an observer, in this case, the satellite is the source and the receiver is the observer. As the frequency of the signal is known, the simplistically Doppler shift can be used to determine velocity as seen in Equation 29.

Equation 29 Doppler Shift Equation (Johnson, et al., 2000)

A vehicle's body slip angle can be defined as the difference between a vehicle's heading and direction of travel, both GPS techniques utilise this definition to determine the body slip angle. The velocity determined from a single GPS can be directly used in combination with yaw gyro estimated vehicle heading to calculate the vehicle sideslip via the use of Equation 30. Alternatively the use of two laterally mounted GPS antennas provide heading and yaw angle, so the vehicle's body slip can be directly measured with use of Equation 31. Unfortunately, the low update rate of GPS receivers ~ 1-10 Hz is not sufficient for vehicle safety systems (Ryu, et al., 2002). In order to overcome the low update rate of the GPS receivers Bevly et al., and Beiker et al propose integration of the GPS data and inertial measurements via the use of a Kalman filter. An example of a vehicle setup and 2D sensor diagram can be seen in Figure 23. It is clear to see in Figure 23 the how the Inertia sensors and GPS sensors feed into the Kalman Filter to determine the vehicle states.

Equation 30 Body Slip Angle using GPS (Bevly, et al., 2006)

Equation 31 Body Slip Angle Using Two GPS Antenna's (Beiker, et al., 2006)

This item has been removed due to 3rd party copyright. The unabridged version of the thesis can be viewed in the Lanchester Library Coventry University.

Figure 23 Example of INS/GPS Setup for Real Time Body Slip Angle Sensing (Beiker, et al., 2006)

Unlike the Kalman filter based body slip angle estimation method detailed previously, the Kalman filter used by Bevly et al., is a kinematic Kalman filter. The state space form for the kinematic Kalman filter can be seen Equation 32.

Equation 32 State Space Form of Kinematic Relationships (Bevly, et al., 2006)

This item has been removed due to 3rd party copyright. The unabridged version of the thesis can be viewed in the Lanchester Library Coventry University.

The Kalman filter (applied to Equation 32) is constructed to integrate the yaw rate gyro measurements between the GPS measurements or during GPS outages, to increase the previously mentioned low update rate of the GPS and ensure body slip angle calculation even when the GPS antenna has lost signal. The Kalman filter is also designed to estimate the vehicle heading and the yaw rate bias; it consists of both a time and measurement update that occurs at each time step. The time update is based on high order integration and is used primarily to forward estimate the vehicle heading from the yaw rate gyro when the GPS measurement data is not available. The Kalman Filter is designed this way so that it does not use previous potentially inaccurate GPS data from a state that may no longer be current. When the GPS is, functioning

the Kalman filter uses the GPS data in order to estimate the bias on the yaw rate gyro, and removes the estimated bias from the yaw rate gyro signal. The yaw rate gyro bias is removed by the use of the GPS heading plus sideslip measurement (GPS course), which is typically assumed as zero during straight driving. For the single GPS antenna, the body slip angle is determined as the difference between the GPS course and the estimated heading as seen in Equation 33.

Equation 33 Body Slip Angle via GPS (Bevly, et al., 2006)

As previously mentioned the dual GPS antenna technique can be used to determine the vehicle heading. The inertial sensors can be combined with multiple GPS measurements and with the use of Equation 34. The Kalman filter can then be applied to this equation in order update the estimates, but unlike the single antenna, method body slip angle is a direct output.

Equation 34 Dual GPS Kinematic Estimator (Bevly, et al., 2006)

Bevly et al and Beiker et al, validate the dual GPS antenna technique against physical test data. It is clear to see from Figure 24, Figure 25 and Figure 27 that the body slip angle has been successfully sensed at various speeds and during transient manoeuvres using GPS. Figure 24 and Figure 25 also show that yaw rate can also successfully be estimated.

Although the use of GPS to estimate body slip angle is successful, the biggest limitation to this process is GPS sensor reliability. Beiker et al, states, “functions that rely on GPS information must have a backup, which could be realized using inertia sensors only” (Beiker, et

al., 2006). With this in mind the Kalman filter aims to ensure that during GPS signal loss the estimation remains accurate by integration of the yaw gyro. But the theoretical performance estimation provided by Bevy et al., shows that if a one GPS antenna is switched off (from a dual antenna system) the accuracy of the estimation continues to decrease as time increases, due to the increase in heading error from integrating the yaw gyro, this can be seen in Figure 26. Figure 26 shows the covariance analysis results for the estimated body slip angle for two dual antenna techniques one which uses the lateral acceleration and one which doesn't, at 50 seconds a GPS antenna is switched off, so that beyond 50 seconds accuracy of a single GPS antenna can be determined (Bevly, et al., 2006).

It is interesting to note that with the single GPS antenna technique the loss of signal could lead to significant estimation errors, due to extended integration of the yaw gyro to estimate the heading by the Kalman filter. It is worth noting that Bevy et al., has not verified the effectiveness of the single GPS antenna technique against physical test data.

Figure 24 Comparison of Measured and Estimated Sideslip Angle and Yaw rate During 8 m/s hard cornering manoeuvres (Bevly, et al., 2006)

Figure 25 Comparison of Measured and Estimated Sideslip Angle and Yaw Rate during a 32 m/s Lap Around The Test Track (Bevly, et al., 2006)

This item has been removed due to 3rd party copyright. The unabridged version of the thesis can be viewed in the Lanchester Library Coventry University.

Figure 26 Covariance Estimate of Sideslip Angle Measurement at 8 m/s (Bevly, et al., 2006)

This item has been removed due to 3rd party copyright. The unabridged version of the thesis can be viewed in the Lanchester Library Coventry University.

Figure 27 Body Slip Angle during Lane Change Manoeuvre (Beiker, et al., 2006)

2.5.2 Real Time Body Slip Angle Sensing Using Optical Sensors

Currently a more commonly used method of real-time body slip angle sensing is the use of optical sensors, the use of optical sensors to determine body slip angle is a far simpler approach to body slip angle estimation than that seen with the INS/GPS sensing. For the majority of estimation techniques researched that compare physical data to estimation results optical sensors will have been used to measure body slip angle.

Optical sensors can be used to determine a vehicle's lateral and longitudinal velocity, which can be used to determine slip angle by use of Equation 35. Simplistically an optical sensor determines velocity by the modulation of a photocurrent that is created due to the change in the projected surface through an optical grating on a photoelectric detector. The sine wave generated due to the modulation is used to determine the speed via the use of Equation 35 (Corrsys Datron, n.d.)

Equation 35 Slip Angle Calculation from Optical Sensors

Equation 36 Frequency of Sine Wave to determine Velocity (Corrsys Datron, n.d.)

Typically, a vehicle with optical sensors to determine body slip angle, will have a sensor on the front and the rear of the vehicle although they can be side mounted. The use of two sensors or more, will also allow the vehicle's yaw rate to be determined, as the yaw rate can be defined as the difference in lateral velocity at the front and rear axle. An example of ideal sensor locations can be seen in Figure 28, the distance from the road surface is dependent on the specific sensor. It is worth noting that optical sensors can also be mounted on the wheels to determine the tyre slip angle.

This item has been removed due to 3rd party copyright. The unabridged version of the thesis can be viewed in the Lanchester Library Coventry University.

Figure 28 Optical Sensor Mounting Locations (Kistler, 2014)

It is worth noting that the slip angle will be different at different points on the vehicle, so the velocities from the optical sensor will need to be corrected to reflect the body slip angle at the vehicle's CG location. The lateral and longitudinal velocity at the vehicle centre of gravity can be calculated using Equation 37 Longitudinal and Lateral Velocity at CG

Equation 37 Longitudinal and Lateral Velocity at CG

This item has been removed due to 3rd party copyright. The unabridged version of the thesis can be viewed in the Lanchester Library Coventry University.

Although optical sensors are widely used in the automotive industry a key limitation is that they require road surface features to be stochastically distributed and require no sudden changes in the road surface in regards to structure to remain accurate (Corrsys Datron, n.d.).

2.5.3 Comparing INS/GPS against Optical Sensors

With INS/GPS units becoming more and more popular due to affordability and ease of use (as they do not typically require external rigs for attachment like optical sensors), several investigations have been carried out comparing the performance of INS/GPS units against optical sensors.

Beiker et al, (Beiker, et al., 2006) who propose the use of INS/GPS units for determining body slip angle show that the INS/GPS sensors are more responsive and less noisy than optical sensors but less accurate. This can be seen respectively by the delay in body slip angle and the difference in magnitude for a lane change manoeuvre seen in Figure 27.

Optimum G (Optimum G: Vehicle Dynamics Solutions, 2010), carried out an investigation, which compares the use the Corrsys Datron S350 Slip angle sensor, the Corrsys Datron SHR slip angle sensor, the Corrsys SFII Tyre Slip tyre slip angle sensors, which are commonly optical sensors against the GeneSys ADMA-G which is an INS/GPS unit. Optimum G, initially compares the SHR and S350 optical sensors against each other, both fundamentally work the same way and use halogen bulbs to illuminate the road surface, the key differences are in their internal filtering and their overall angle resolution, with the SHR having an angle resolution of $\pm 0.01^{o}$ and the S350 having an angle resolution of $\pm 0.1^{o}$. The longitudinal speed, lateral speed, body slip angle measured from the sensors during a slalom manoeuvre can be seen in Figure 30. Interestingly the SHR sensor [red] with higher resolution produces significantly nosier results, particularly in the longitudinal speed measurement, which may be due to the higher magnitude when compared to the lateral speed and the internal filtering. The overall difference in noise is further emphasised when looking at the derivative of body slip angle from both sensors, seen in Figure 30. Overall, both sensors seem to produce similar measurements with the S350 measuring on average +0.29 degrees higher body slip angle (Optimum G: Vehicle Dynamics Solutions, 2010). The SHR has a better time response when compared to the S350 but significant gains can be made by modifying the internal filtering to remove noise without losing data fidelity. Due to the noise seen in the SHR the S350 sensor was used for the rest of the investigation.

Figure 29 Comparison between Corrsys Datron SHR and S350 sensors for Longitudinal Speed, Lateral Speed, Slip Angle and Steering Angle Measurements (Optimum G: Vehicle Dynamics Solutions, 2010)

This item has been removed due to 3rd party copyright. The unabridged version of the thesis can be viewed in the Lanchester Library Coventry University.

Figure 30 Derivative of Body Slip Angle Comparison, SHR vs. S350 sensors (Optimum G: Vehicle Dynamics Solutions, 2010)

The next part of the investigation carried out by Optimum G involves comparing body slip angle sensing using; 2 x S350 sensors, 1 x s350 Sensor with a GYR3 gyro from Texys, the GeneSys ADMA-G, 2 x SF11 tyre slip angle sensors and 1 x S350 sensor with yaw rate from the ADMA-G. The results from this investigation can be seen Figure 31.

It is immediately clear to see that ADMA-G sensor alone shows the least amount of noise and all the sensing techniques seem to correlate relatively well with each other except for the SFII sensors, this may fundamentally due to the fact that they are mounted to the wheel which is subject to larger disturbances. It is interesting to see that the body slip angle is consistently delayed and underestimated with the use of the S350 sensor and gyroscope, which is not the case with the S350 sensor and the ADMA-G, this may be due to the inertia of the gyroscope (Optimum G: Vehicle Dynamics Solutions, 2010). When comparing the two A350 sensors, the S350 sensor with ADMA yaw rate and the ADMA sensed body slip, it is clear to see that the two S350 sensors and the S350 sensor with ADMA yaw rate almost identically measure body slip angle (including noise), whereas there is a clear variation with the ADMA unit alone during the final section of the plots, this suggests that the variation is due to ADMA unit's ability to measure, either the lateral and longitudinal velocities. It is also interesting to note that the ADMA sensor seems to show on average a marginally lower time response delay, which can be seen when comparing the body slip angle, plots to the steering angle.

Overall it's clear to see that the S350 sensors with or without a yaw gyroscope and the ADMA-G sensor are both successful in measuring with body slip angle with significant accuracy, but the optical sensors exhibit more noise and a marginally higher time delay, this further confirms the results from Beiker et al.

Figure 31 Slip Angle Comparison between various Body Slip Angle Sensors (Optimum G: Vehicle Dynamics Solutions, 2010)

2.5.4 Doppler Velocity Sensors

The use of Doppler velocity sensors to determine longitudinal vehicle ground speed has been widely investigated, but their use for body slip angle measurement has not. As the body slip angle can be defined as the arctangent of lateral velocity over the longitudinal velocity as seen in previously, it seems that there may be potential to use Doppler velocity sensors to also measure the vehicle longitudinal speed and therefore slip angle. Doppler velocity sensors use the Doppler Effect to determine velocity, similar to the GPS systems previously mentioned.

The Doppler systems proposed by Ditchi et al., (Ditchi , et al., 2002), Richardson et al., (Richardson, et al., 1982), Kidd et al., (Kidd, et al., 1991) and Baba et al., (Baba, et al., 1979) all use radio waves or microwaves as source signals. The source waves are emitted from the sensor to the ground at an angle; the signals are then reflected from the ground surface and returned to the sensor, the Doppler shift of the returned waves can be used to determine the velocity. This can be done using Equation 38, the proposed vehicle setup can be seen in Figure 32.

Equation 38 Doppler Shift Frequency From Ground Reflections (Kidd, et al., 1991)

Figure 32 Using Under Vehicle Mounted Doppler Velocity Sensors to Measure Vehicle Velocity (Kidd, et al., 1991)

Baba et al., (Baba, et al., 1979) propose the use of Doppler velocity sensors in order measure the ground speed for ABS systems. The results show that the Doppler velocity sensors are beneficial and can be successfully implemented into ABS systems. This emphasises the fundamental capabilities of Doppler velocity sensors, in that they can accurately determine velocity and they can be used in vehicle safety systems.

The key benefit for Doppler velocity sensors is robustness; this is highlighted by Richardson et al., (Richardson, et al., 1982), who proposes the use of Doppler velocity sensors to determine the ground speed of tractors, which is typically difficult using conventional wheel speed sensors due to wheel slippage. The results showed that the ideal method of measuring the ground speed was via the use of dual beam Doppler velocity sensors with a narrow radar beam. Richardson et al also state that the optical sensors were not accurate due dust obstruction, crop motion and wind speed (Richardson, et al., 1982).

Overall current research suggests that Doppler velocity sensors could show benefits over optical and GPS real time body slip angle sensing techniques, as they are highly robust on varying road surfaces, which doesn't seem the case for optical sensors and are not susceptible to signal drop out like GPS. Further investigation would be required in order to determine if Doppler velocity sensors could be utilised on commercial road vehicles, as these benefits have been assessed on slow moving agricultural vehicles.

2.5.5 Laser Doppler Velocity Sensors

As research has shown that radar based Doppler velocity sensors could be beneficial, laser Doppler velocity sensors (laser Doppler velocimeters), could prove even more beneficial.

The laser Doppler velocity sensors work by splitting the coherent laser beam into two separate beams and intersecting them, the coherence of the laser means that at the point of intersection interference fringes are created. In regards to ground vehicle speed, the sensor should be designed so that the split laser beams intersect at the road surface, as the road surface travels through the light and dark regions of the interference fringes, the features in the road surface reflect the light back to the sensor. Due to the intersection of the beams, the light returned from each beam will have a Doppler shift in opposite directions, i.e. the frequency of the returned light from one laser will be less than the source frequency, and the frequency of the returned light from the other beam will be higher than the source frequency. Due to the coherence of the laser, the sensor will detect both light intensity frequencies at the same time. The returned intensity will therefore be sinusoidal due to the inference of the two returned frequencies, causing a fluctuation in the measured intensity. As the fringe widths are known for a particular setup and the returned light intensity frequencies are measured, the velocity of the road surface can be calculated, as the velocity is the fringe spacing multiplied by the frequency of the returned intensity. (Measurement Science Enterprise, Inc, 2014)

Phillips, (Koninklijke Philips N.V., 2014) state that particular benefits of their Doppler velocity sensor include;

- *Accurate Speed Measurements over 360 km/h*
- *Nominal Working Distance from mm's up to meters*
- *Working range from 30 to 60% of nominal distance*
- *Accuracy better than 0.01%*
- *Resolution from wavelengths up to cm's*
- *Works on Virtually all Surfaces*
- *Insensitive to Environmental light*
- *Robust to Smoke mist or dust*

(Koninklijke Philips N.V., 2014)

It is because of the clear high accuracy and robustness that laser Doppler velocity sensors have been used for used for a variety of purposes in the automotive and aerospace industry such as investigating fluid flow in engines downsized engines (Galmiche, et al., 2013), and measuring subsonic jet turbulence as early as 1969 (Huffaker, et al., 1969). When comparing laser Doppler velocity sensors with current body slip angle measurement techniques it clear that laser Doppler velocity could be a viable alternative. Laser Doppler velocity sensors are advantageous over optical sensors as they generally have a higher accuracy, typically can work at higher speeds and robust against external disturbances such as dust. It is worth mentioning that although the laser Doppler velocity sensors are more accurate this may not always be beneficial without adequate filtering as previously seen when comparing the Corrsys Datron S350 and SHR sensors. The laser Doppler velocity sensors are also advantageous when compared to GPS, as they are not susceptible to signal drop out and there are potentially more affordable. A robust study would need to be carried out to determine the cost benefit of laser Doppler velocity sensors, but initial research proves promising as laser Doppler velocity sensors are increasingly being used in everyday technology such as computer mice. It is also interesting to note that Koninklijke Philips has recently filed a patent for the use of laser Doppler velocity sensors in order to derive, vehicle's side slip, slip angle, front and rear tire slip angles, yaw rate and lateral acceleration rate (Meng, 2014). This further highlights that laser Doppler velocity sensors are a suitable means of determining direct real time slip angle.

2.5.6 Existing Controllers that Use Doppler Velocity Sensors

Doppler velocity sensors have been widely implemented to measure ground velocity due to their robustness in a variety of situations; it is because of this they are used on agricultural vehicles, as measuring true ground speed from wheel speed sensors proves difficult due to longitudinal wheel slip.

The recent push in the development and research of autonomous all-terrain vehicles has led to the use intelligent vehicle controllers that utilise doppler velocity sensors combined with intelligent vehicle models to determine previously unknown vehicle states. Lhomme-Desages et al (Lhomme-Desages, et al., 2012), successfully implement a low cost radar Doppler velocity sensor to measure the true ground speed of a small four wheeled rover. Lhomme-Desages et al propose the use of a Doppler velocity sensor combined with a vehicle model in order to accurately determine actual ground speed and individual wheel slip.

Lhomme-Desages et al, attach the low cost Doppler velocity sensor to the front of the rover at a 20-degree angle, which is determined to produce an acceptable relative error (10%). Figure 33 shows the doppler velocity sensor frequency acquisition process; initially a low pass filter which helps eliminate high frequency data from the signal, the signal is then amplified and passed through a pass band filter than limits the signal frequency so that it is between 3Hz and 80Hz. The data is then Fast Fourier transformed so that the power spectrum and therefore the change in frequency can be determined. It is interesting to note that even after the filtering, the signal is still noisy, this can be seen when looking at Figure 34. Fundamentally Lhomme-Desages et al attribute this error to the beam width of the radar, and although a brief comparison of high accuracy sensors is carried out, where it is clear to see that the sensor accuracy increases with an increase in base frequency and a decrease in beam width, (as seen when looking at Table 4). Lhomme-Desages et al opt to use the MDU113O because of its weight and cost. In order to increase the accuracy of the measured ground speed, Lhomme-Desages et al propose fusing the Doppler velocity sensor measurements with accelerometer measurements via the use of a Kalman filter, which significantly reduces the noise in the signal.

Lhomme-Desages et al use the accurately measured velocity to control the longitudinal velocity of the vehicle by controlling the wheel slip rate. The controller is designed to estimate the wheel soil interaction so the system can determine the desired torque to the wheels. Overall Lhomme-Desages et al successfully implement Doppler velocity sensors into a control system to control vehicle states.

Figure 33 Doppler radar Frequency Acquisition Process (Lhomme-Desages, et al., 2012)

Figure 34 Radar signal after amplification (a) Voltage vs Time (b) Spectral power density (Lhomme-Desages, et al., 2012)

Table 4 Radar Comparison (Lhomme-Desages, et al., 2012)

2.6 Existing Electronic Stability Control Systems Utilising Body Slip Angle

Whether or not body slip angle is estimated or measured, the data can only be utilised if successfully implemented into a vehicle controller. Although current production vehicles do not have the capability to directly measure slip angle, slip angle is a required input into current electronic stability systems. Zanten states that the main task of ESC is to "limit the slip angle in order to prevent vehicle spin" (Zanten, 2000) and another task is to "keep the slip angle below the characteristic value to preserve the yaw moment gain" (Zanten, 2000). As body slip angle is not measured on current production vehicles it has to be estimated, but as previously mentioned estimated body slip angle is not always reliable, therefore control systems that solely rely or heavily rely on body slip angle estimation are not robust enough for production vehicles. In order to achieve the aforementioned tasks of ESC and successfully utilise the estimated body slip angle, intelligent control systems are created.

Current ESC controllers can fundamentally be split into a two system hierarchy, as previously seen in section 2.2, the upper system determines the vehicle dynamic response, i.e. the desired vehicle motion and the lower system implements the desired vehicle motion via brake proportioning. The initial system that determines the vehicle response is where the body slip angle estimation is intelligently combined with yaw rate estimation to determine the vehicle's current and desired behaviour, a simplified block diagram of an ESC system can be seen in Figure 35. Simplistically Figure 35 shows that the car motion controller determines what yaw moment needs to be generated based the vehicle's body slip angle and yaw rate. The car motion controller then passes that information down through various other controllers until the yaw moment is implemented by the actuation of the vehicle brakes.

The intelligent use of body slip angle is in the car motion estimation. The car motion estimator determines the vehicles current behaviour, by using an observer based on a simple full car model. Unfortunately, due to the fundamental setup of the observer the body slip angle cannot be determined if the tyres are free rolling, this is because the longitudinal tyre slip used to determine the relationship between lateral force and longitudinal force, is too small. When the observer cannot be used, a more simplistic pseudo integration technique to determine body slip angle is used. The multiple methods to determine body slip angle leads to variations in accuracy depending on the vehicle's current state. In order to combat the variation in accuracy, the controller is set up as a cascade controller where the outer (master) loop is the previously

described body slip angle controller and the inner (slave) loop is a model following control based yaw rate controller. The inner loop, which utilises the measurable yaw rate (from the yaw rate sensor), provides an increase in accuracy of the outer loop. It is worth noting that the inner controller is based on a fixed model that will become inaccurate over time due to aging of the vehicle and its components, therefore various compromises in the accuracy of the inner model need to be made in order for the model to remain robust over the lifetime of a vehicle (Zanten, 2000).

Although the implementation of estimated body slip angle into an electronic stability control system is successful, it is clear that the uses of direct real time slip angle sensing, could enhance the accuracy and robustness of an electronic stability control system.

Figure 35 Simplified Block Diagram of ESC Control (Zanten, 2000)

2.7 Body Slip Angle based ESC System Proposal

From the research carried out it is clear to see that direct measurement of body slip angle could prove beneficial for electronic stability control systems, with this in mind the following ESC system is proposed.

As Doppler velocity sensors combined with intelligent controllers have been successfully implemented for robust vehicle velocity measurements, as seen in section 2.5.6, the proposed body slip angle ESC system will consist of laser Doppler velocity sensors. Although expensive, the use of laser technology is chosen due to the high accuracy available as a function of the laser's beamwidth and frequency properties. The higher accuracy, which would be necessary for the application on consumer vehicles, may lead to highly noisy results, with this in mind sensor fusion with an accelerometer is proposed similar to that as seen in sections 2.5.3 and 2.5.6.

The proposed system consists of a minimum of six laser Doppler velocity sensors, split into three pairs, a pair on each axle and one pair in the centre of the vehicle, or as close to the vehicle's centre of gravity. The two sensors in each pair will allow for the lateral and longitudinal velocities at each position. This will allow for robust slip angle measurement, but also help determine individual tyre slip angle, yaw rate and if the vehicle is understeering or oversteering. The proposed ESC system will also require the use of a hand wheel position sensor, which is a typical component of a traditional ESC system. The hand wheel position sensor could be omitted, with additional Doppler velocity sensors mounted so that they would rotate with the steered road wheel, an example of the sensor positioning options can be seen in Figure 36. At each of the sensors, the slip angle can be determined, on the proposed sensor positions (purple) the slip angle at their given positon can be calculated with Equation 39. Typically, the body slip angle will be determined by the centre sensor, but the data from the other positions can be translated to the position of the centre sensor to verify the body slip angle. Equation 39 can also be used on the wheel sensor but as this rotates with wheel, the wheel slip angle will be determined form this sensor.

Equation 39 Slip Angle Calculation

As previously mentioned the proposed sensor set up will allow for robust yaw rate measurement, the yaw rate can be determined from the difference in lateral velocity at the front and rear sensors. The yaw rate, body slip angle and steered wheel angle can be used to determine the slip angles at the individual wheels, which in turn can be used to determine whether the vehicle is understeering or oversteering, based on the following relationships:

If the vehicle is understeering front axle slip angle > rear axle slip angle

If the vehicle is oversteering front axle slip angle < rear axle slip angle

The longitudinal velocity at each axle will also help verify if the wheels on the axle have locked, overall this data from the sensors will provide sufficient information to an electronic stability control system.

A central computing unit will be used to process the sensor data in regards to sensor filtering and fusion and be the primary controller for the electronic stability control system. The processed data will then be used to determine the vehicle's current behaviour and desired behaviour and determine what brake actuation may be required to achieve the desired vehicle behaviour. A block diagram breakdown of the proposed electronic stability control system can be seen in Figure 37. If the proposed system were to be implemented significant testing, refinement and validation would need to be carried out, in order to ensure that the ESC system performed successfully for a variety of undesirable situations. It is highly likely that further refinement would need to be carried out on the sensor position and orientation, in order to achieve accurate results.

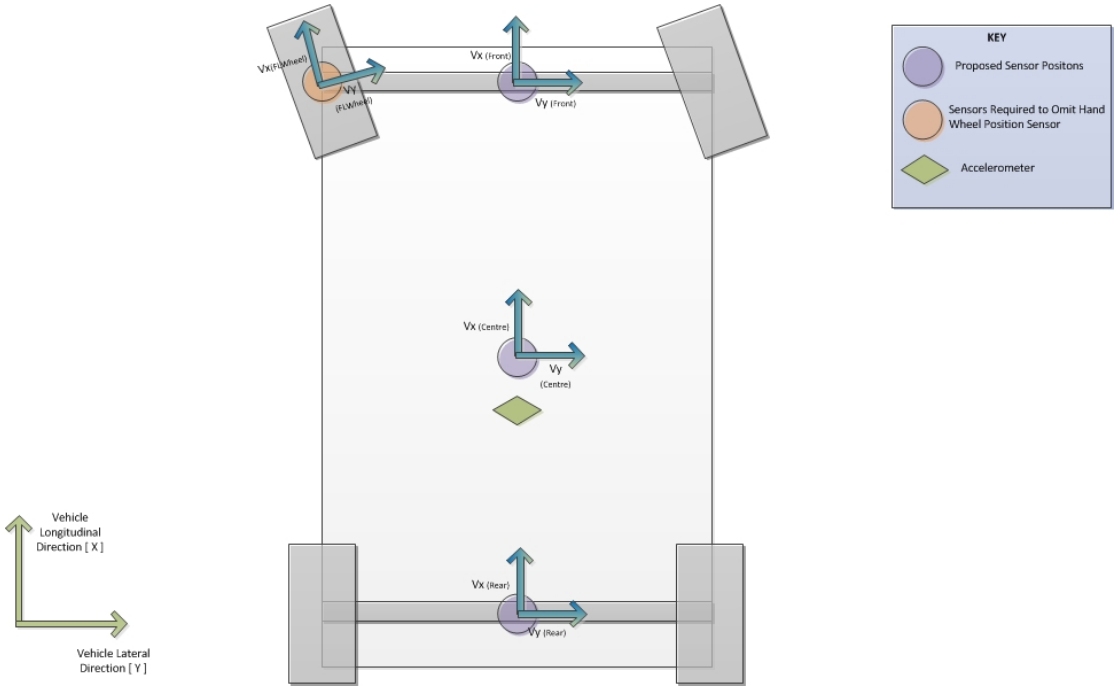

Figure 36 Proposed Sensor Positions.

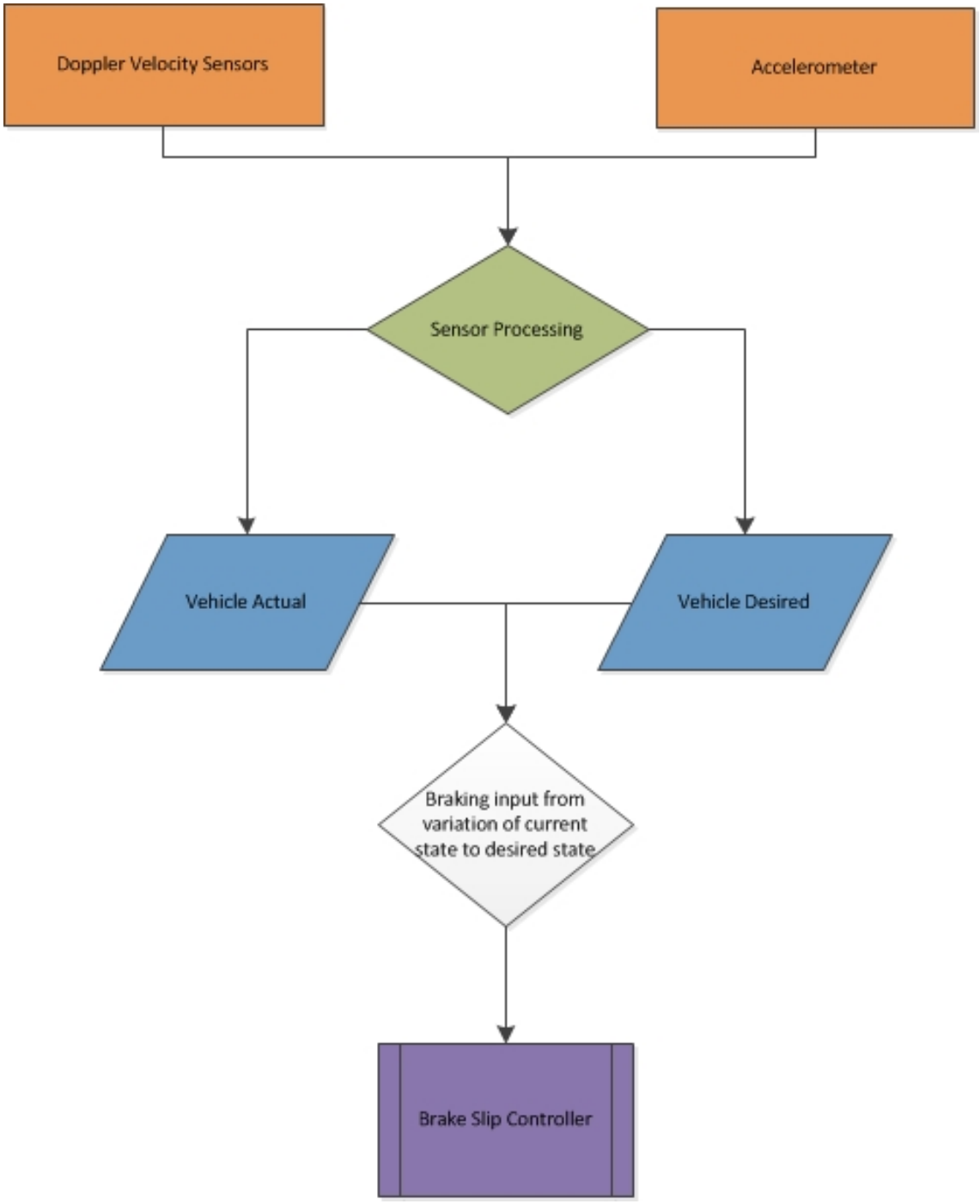

Figure 37 Block Diagram of proposed Controller Logic

2.8 The Benefit of Real Time Slip Angle Sensing

Real time slip angle sensing fundamentally is beneficial over slip angle estimation as real time slip angle sensors are not susceptible to errors in vehicle parameters such as vehicle mass and cornering stiffness and therefore are inherently more robust, slip angle sensors are also less susceptible to consistent sensor errors due to sensor integration. The use of any of the previously mentioned methods could prove highly beneficial to vehicle control.

The real benefit to direct real time slip angle sensing is the use of this information in vehicle safety systems such as electronic stability control (ESC) systems. Zanten (Zanten, 2000), states that ESC has two main tasks, these involve limiting the body slip angle so that the vehicle doesn't spin, and ensuring that the body slip angle is low enough to allow for yaw moment gain. If the body slip angle increases, the yaw moment gain decreases and therefore the overall manoeuvrability of the vehicle diminishes. This being true, as previously mentioned the body slip angle is estimated and it cannot always be estimated accurately, with this in mind the control systems fundamentally aim to target a desired yaw rate, as yaw rate can be easily measured. The control systems typically consist of an inner yaw rate control loop and an outer body slip angle control loop (Zanten, 2000) as it is a necessity to limit the body slip angle. As the body slip angle control is an essential using real time slip angle sensors to determine actual body slip, may allow for the use of direct body slip angle control systems, which may prove beneficial over yaw rate controlled systems. With this in mind, Multi Body Simulations have been carried out to determine the potential gain of body slip angle controlled stability control systems.

3.0 MULTI BODY SIMULATION

The following Multibody simulation has been carried out using SIMPACK MBS software. Multibody Simulation is widely used and an accepted method in the automotive industry for vehicle dynamics analysis. Multi body simulation is increasingly being used as alternative to physical vehicle testing

3.1 Test Vehicle Evaluation

The vehicle data used for the simulation is from a full vehicle MSC ADAMS model, which has been provided by Coventry University. The vehicle being modelled is a well-accomplished high performance rally vehicle, and therefore varies from a traditional production vehicle but it is still suitable for this investigation. The vehicle is a four-wheel drive manual transmission vehicle, with McPherson front suspension and multi-link rear suspension. The vehicle is considerably lighter than a traditional production vehicle, with the vehicle's total mass being 1440.4 kg. The vehicle's dynamic set-up in regards to springs, dampers and anti-roll bars also reflect that the vehicle has been set up for performance. A production version of this vehicle exists which has a similar suspension type and geometry and therefore the kinematics of the vehicle should not be too dissimilar to that of a production vehicle. Unfortunately, due to confidentiality agreements further information about this vehicle has been omitted. Fundamentally, the vehicle was chosen as it was the only comprehensive source of vehicle data that was made available for this investigation, and as the simulation sets out to determine the differences in vehicle behaviour, (not absolute values), it is appropriate for the investigation.

Although the model provided was created in MSC ADAMS MBS software, SIMPACK was used for this particular investigation due to the ease of control system creation within SIMPACK and the ease of co-simulation with other software packages if required. In order to create a model in SIMPACK, data such as hard points, mass and inertia and the steering gear ratio were taken from the ADAMS model.

3.2 MBS Model Evaluation

The MBS model has been created in SIMPACK; the data used to create the model has come from ADAMS model data that was made available by Coventry University. The simulation, as previously mentioned is fundamentally focusing on differences and not absolute values; therefore, some appropriate changes have been made to the model fidelity in order to ease modelling, simulation time and analysis of results. The main simplifications in model fidelity include; the use of all rigid components (no flexibility in the individual parts), the removing compliances, the removing the powertrain system and replacing them with arbitrary in hub electric motors, and ignoring aerodynamic effects. The model consists of McPherson front suspension, multi-link rear suspension, a simple steering system, electric motors and magic formula tyre models.

The McPherson front suspension can be seen in Figure 38. The suspension has been modelled as three components on each side, a knuckle, a lower wishbone and a strut rod with an anti roll bar between each side. All the components have non-compliance joints between them. The front spring and damper act between the strut rod and the front knuckle and the anti roll bar attaches to the lower wishbone. The front springs and dampers have non-linear behaviour whereas the anti roll bar exhibits linear behaviour; the nonlinear behaviour includes the behaviour of spring aids and rebound springs. The key differences between the MBS and model and the physical vehicle will be the compliance in the McPherson suspension system in the form of bushes and ball joints. The bushes and ball joints are key components that are commonly tuned in the vehicle engineering process to modify the vehicle's dynamics and therefore will effect the over all suspension movement, for example bushes might be tuned to modify the bump steer characteristic, or modify the longitudinal tyre movement during harsh braking. The compliance in the front suspension has not been modelled, as they are infamously difficult to model due to complexity of modelling the behaviour of rubber and are not necessary for the investigation, as absolute correlation and absolute values are not required. The non-compliance front suspension will still reflect the general behaviour of McPherson suspension and will be suitable for stability analysis.

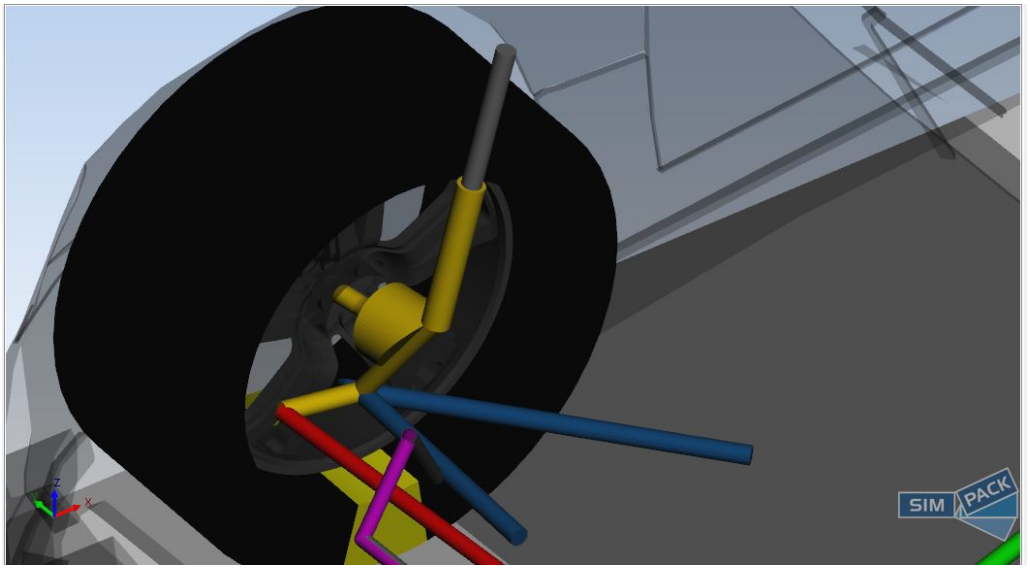

Figure 38 McPherson Front Suspension as modelled SIMPACK

The multi-link rear suspension can be seen in Figure 39. Similar to the front suspension, the suspension has been modelled with non-compliance joints. The suspension has been modelled as five components on each side, with an anti roll bar between each side. The four suspension components consist of a knuckle, a strut rod, a toe-link, a lateral link and a trailing arm. The rear spring and damper are both non-linear and act between the rear knuckle and strut rod, and the anti roll bar has linear stiffness and damping and is connected to the knuckle. As with the front suspension, the main variation in the modelled rear suspension when compared with the physical vehicle will be in the compliances, and similar to the front suspension, this variation is considered as appropriate loss in fidelity for the investigation.

The steering system can be seen in in Figure 40. The steering system consists, of a steering wheel and upper column, a lower column, a steering rack and two track rods. As with the other systems, the steering system does not have compliant joints, but the system has non-linear rack stops that increase in stiffness and damping towards the rack travel approaches a maximum. The rack stops act between the steering rack and the chassis. The biggest variation between the modelled steering system and the physical vehicle is the omission of power assisted steering (PAS). The power assisted steering typically affects the steering effort required by the driver and can effect the driver's perception of road feel, with this in mind; it has not been modelled, as it is not necessary for vehicle stability simulations.

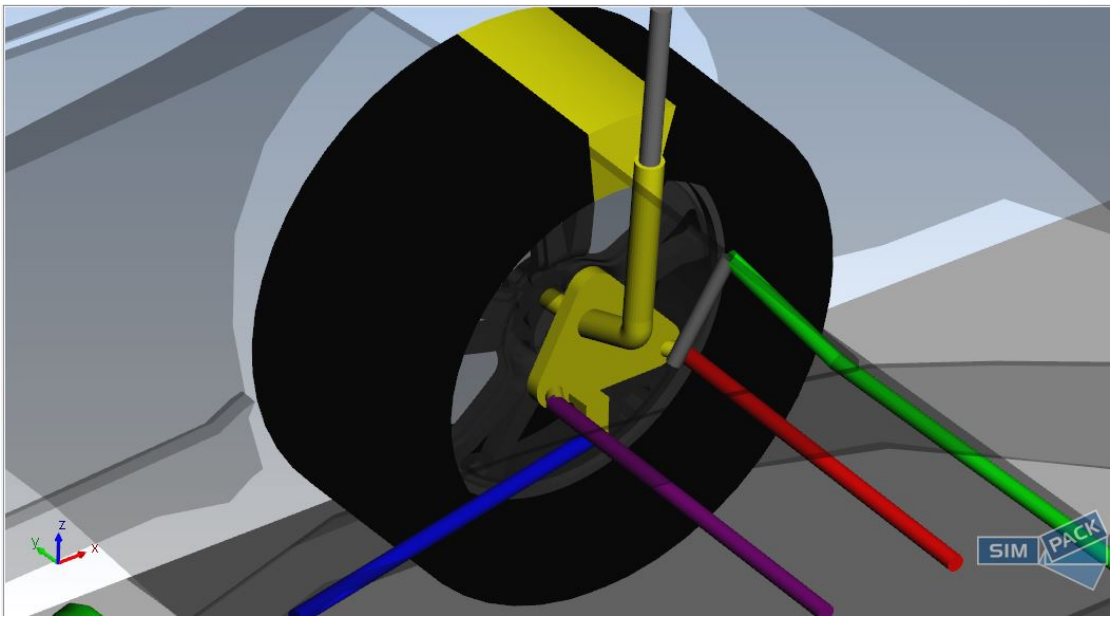

Figure 39 Multi Link Rear Suspension as modelled in SIMPACK

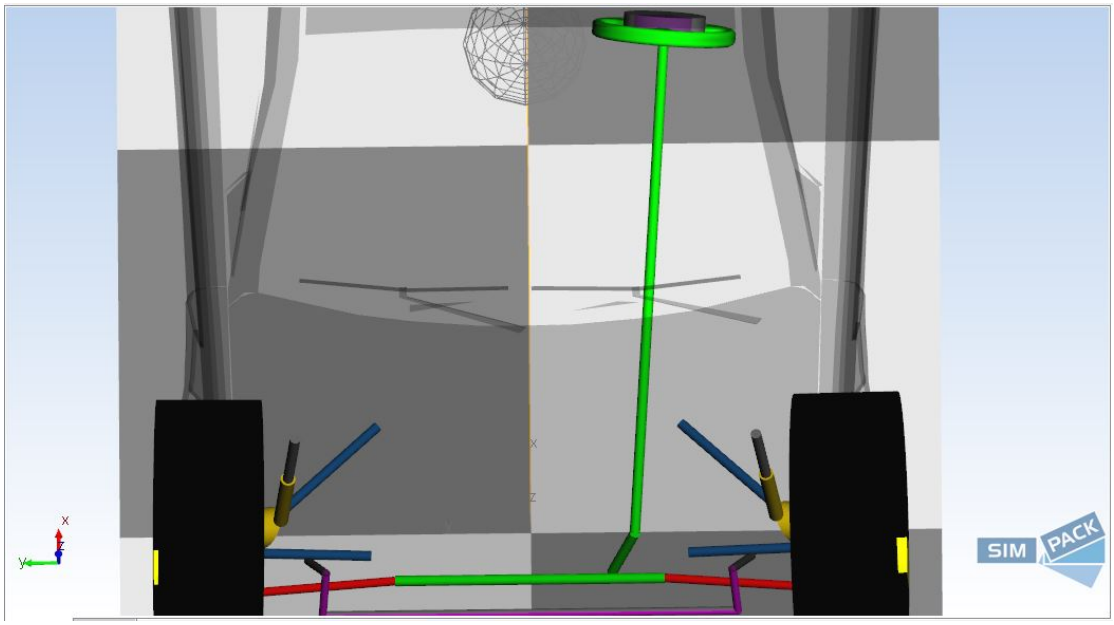

Figure 40 Steering System as modelled in SIMPACK

A key variation between the physical test vehicle and the model is the removing of the powertrain system and replacing the system with in hub wheel motors. This has been done to simplify the modelling and allow for easy implementation of torque vectoring systems for further research. This change should not have a significant effect on the stability of the vehicle and therefore has been considered a suitable variation for the investigation.

The most significant variation between the physical vehicle and vehicle model is the tyres. Due to the difficulty and cost associated with acquiring tyre data, available tyre data provide by Coventry University was used for the simulation. The tyres use magic formula equations to determine the tyre properties for the simulation. The tyres will have a significant effect on the dynamic properties of the model, with this in mind it is unlikely that the model will correlate to the test vehicle, but as the tyres used are considered representative of real tyres, they can still be used for the stability simulations.

It is also worth noting that the aerodynamic properties of the vehicle have not been modelled, although this can have a significant effect on the stability of the vehicle. Modelling the aerodynamic effects accurately would require acquiring a representative surface model for the test vehicle and the use of Computational Fluid Dynamic software, which is out of the scope of the project. The vehicle stability can still be robustly and accurately assessed without the modelling of the aerodynamic data.

3.3 Loadcase Evaluation

Two loadcases have been created in SIMPACK for the vehicle stability investigation, a constant radius loadcase and a sine with dwell loadcase.

3.3.1 Constant Radius

The constant radius loadcase is a quasi-static loadcase that is commonly used to determine the steady state steering and handling characteristics of a vehicle; this test is commonly used in both physical testing and virtual simulation. The loadcase involves the vehicle slowly accelerating around a 30m radius at a rate of 0.1 m/s from 5 m/s to 30 m/s or until a pre specified lateral acceleration has been reached. In order to achieve the radius, the steering control targets a desired curvature based on the 30m radius, as the velocity increases the steering controller increases the steer angle in order maintain the radius. The radius is maintained until the tyres are saturated and the vehicle can no longer maintain the radius. The test can be carried out for either a left or right turn. This loadcase is representative of real world test, and will be suitable to determine the steady state vehicle dynamic properties of the vehicle, which can prove key in understanding the vehicle stability.

3.3.2 Sine With Dwell

The sine with dwell test is a commonly used test for vehicle stability assessment; it is currently used by the European New Car Assessment Programme (Euro NCAP) as an assessment test for electronic stability control performance (Euro NCAP, 2015). With this in mind the test is ideal for simulation as the simulation sets out to determine ESC performance. The loadcase has been created in SIMPACK to the protocol used by Euro NCAP. The protocol is split into two parts, a pre test and the main test; the loadcase is designed so that both parts of the test can be carried out. The pre test is a slow steered test; the steering angle (handwheel angle) increases at a rate of 13.5 degrees per second at a fixed velocity of 80 km/h until a lateral acceleration of 0.5g is reached. The value of the steering angle when the lateral acceleration is reached is termed as "A" which is used for the main test. The main test involves a sine with dwell steering input, which has a frequency of 0.7 Hz and a 500 ms delay (dwell) at the beginning of the second peak, which is applied to the hand wheel. The amplitude of the sine wave is increased from 1.5A in 0.5A increments up to 6.5A or 300 degrees. The initial speed of the loadcase is 80 km/h but the test is carried out off throttle, so that the velocity decreases during the simulation (Euro NCAP, 2011). The loadcase is highly representative of a physical test is deemed ideal for vehicle stability simulations.

3.4 Model Behaviour

In order to determine if the vehicle model is both suitable for vehicle stability investigations and representative of physical vehicles initial analysis was carried out on the vehicle.

3.4.1 Tyre Behaviour

As previously mentioned the tyre models used are not directly representative of the tyres on the test vehicle, but are representative of another set of road tyres. In order to determine if the tyre data is adequate some key plots have been analysed.

Figure 41 shows a plot of longitudinal force vs. longitudinal slip for varying vertical forces. The plot shows that as the longitudinal slip increases, the longitudinal force increases to a peak force, within 0.1 of longitudinal slip and then declines and levels off. The peak force and the longitudinal slip at which the peak force is attained are dependant on the vertical force. The

higher the vertical force, the higher the longitudinal peak force and lower the longitudinal slip at which the peak force is attained. Figure 42 shows that as the vertical force increases the longitudinal stiffness increases, again this is expected behaviour. Overall these plots show expected longitudinal tyre and vertical tyre behaviour.

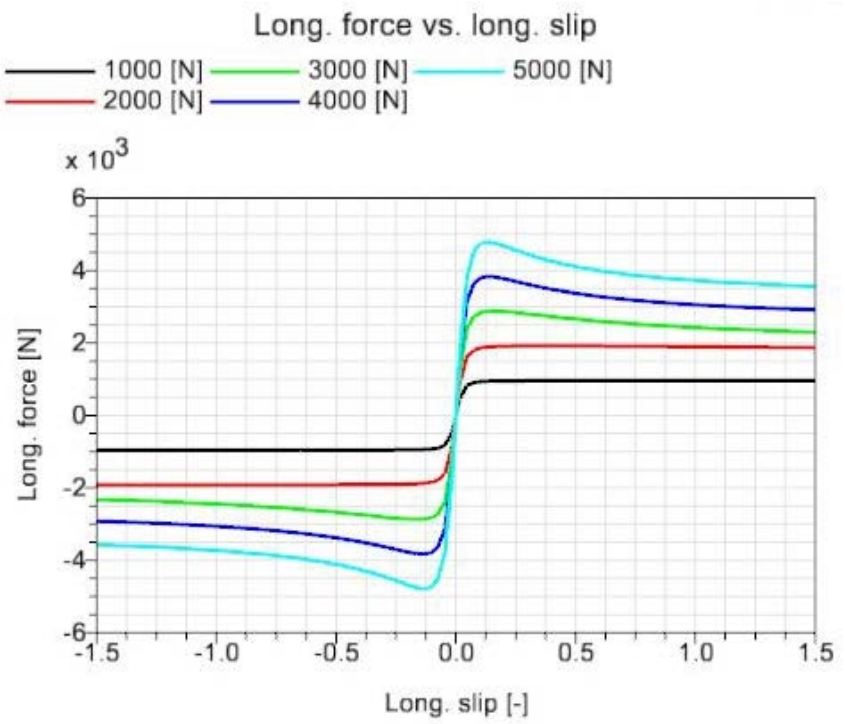

Figure 41 Longitudinal Tyre Force vs. Longitudinal Slip of Tyre used in Modelling (Standard SIMPACK Output

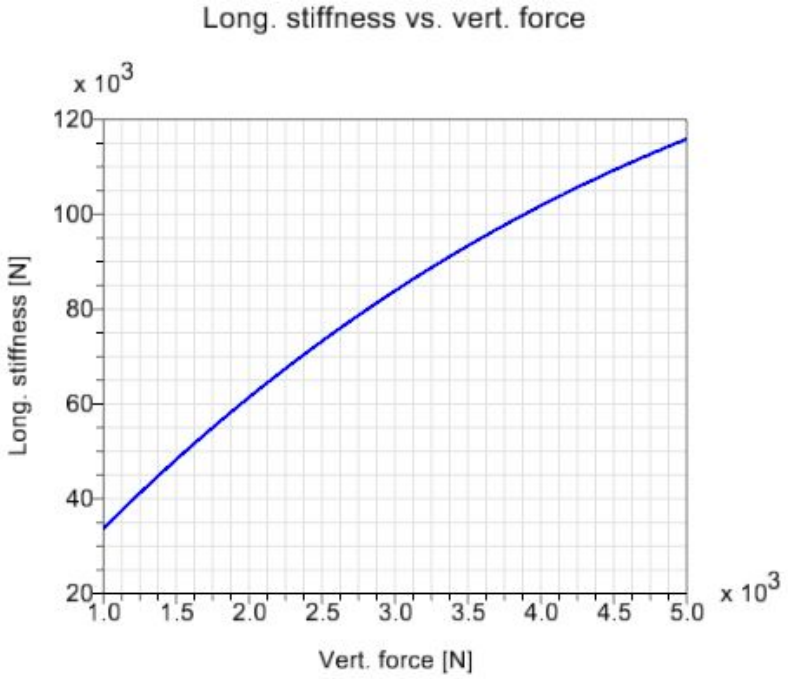

Figure 42 Longitudinal Tyre Stiffness vs. Vertical Tyre Force of Tyre used in Modelling (Standard SIMPACK Output)

Figure 43 shows a plot of lateral force vs. slip angle for varying vertical loads. It is clear to see that as the slip angle increases the lateral force increases to a maximum within about 0.1 radians of slip angle and then levels off just below the peak force. An increase in vertical load increases the peak lateral force and the rate at which that peak is reached. This plot shows expected lateral tyre and vertical tyre behaviour. This plot is particularly important for vehicle behaviour as; " The slope of side force F_y vs. slip angle α near the origin (the cornering or side slip stiffness) is the determining parameter for the basic linear handling and stability behaviour of automobiles" (Pacejka, 2006). Overall from the analysed plots it can be assumed that the tyre behaviour is modelled correctly and suitable for use.

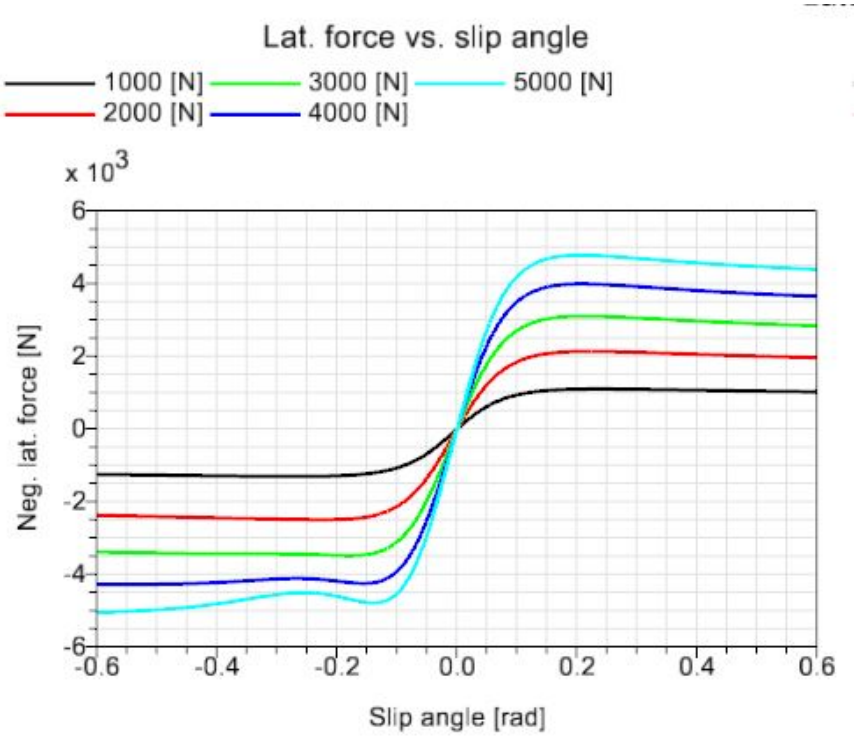

Figure 43 Tyre Lateral Force vs. Slip Angle of Tyre Used in Model (Standard Output of SIMPACK)

3.4.2 Dynamic Behaviour of SIMPACK Model

In order characterise and determine the vehicle behaviour some plots have been analysed from simulation of the constant radius loadcase. The lateral acceleration limit for the simulation was set to 0.85g.

Figure 44 and Figure 45 show, front and rear lateral load transfer vs. lateral acceleration respectively. It is clear to see in both figures that as the lateral acceleration increases the lateral load transfer increases with linearity. This is expected as the when the vehicle is cornering the

inside wheels are loaded as the outside wheels become unloaded. It is interesting to note that there is twice as much lateral load transfer on the rear axle than the front. This suggests that the vehicle cornering ability is largely affected by the rear axle behaviour. Figure 47 shows roll angle vs. lateral acceleration, it is clear to see that the roll angle increases linearly as the lateral acceleration increases, the rate of change of roll angle is about 60 degrees per g. The linearity of the roll angle vs. acceleration plot correlates to linearity of the lateral load transfer plots.

Figure 46 shows yaw rate vs. lateral acceleration, as expected as the lateral acceleration increases, the yaw rate increases; the non-linearity seen is fundamentally due to tyre behaviour.

Overall these plots have helped characterise the steady state vehicle dynamics, the data suggests that the vehicle is behaving as expected, and therefore it can be used for the stability simulations.

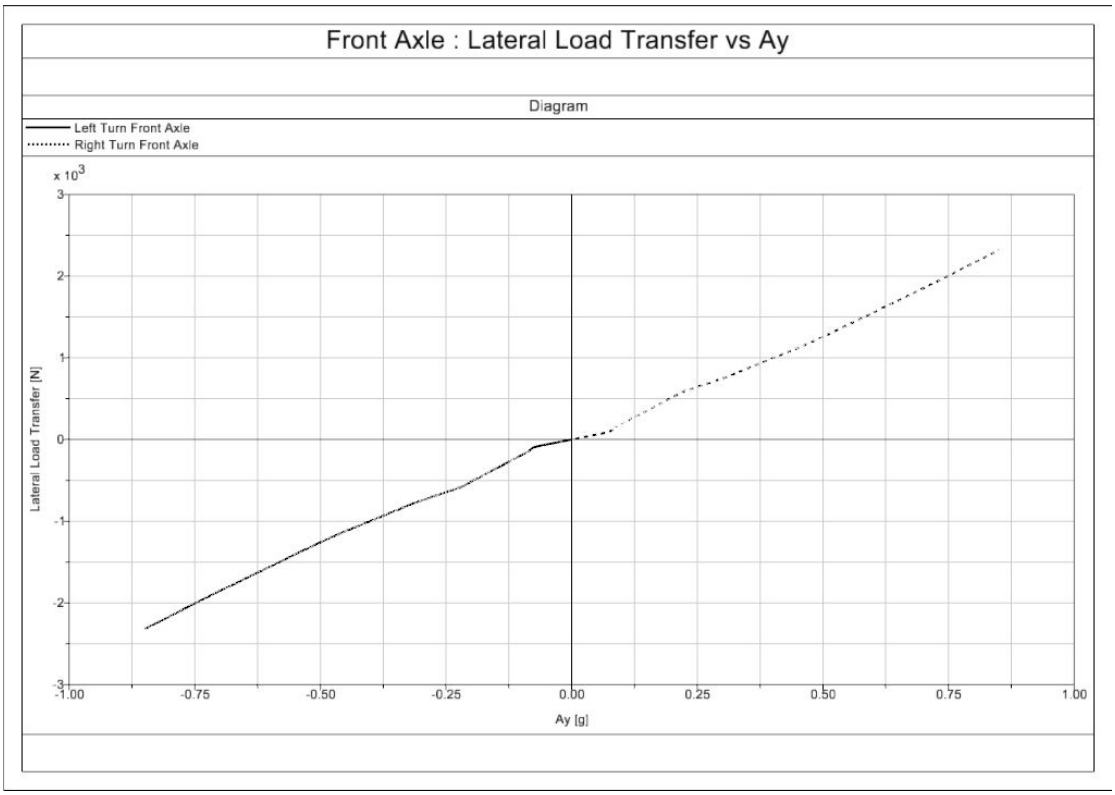

Figure 44 Front Axle: Lateral Load Transfer vs. Lateral Acceleration (g) From Constant Radius Loadcase

Figure 45 Rear Axles: Lateral Load Transfer vs. Lateral Acceleration (g) From Constant Radius Loadcase

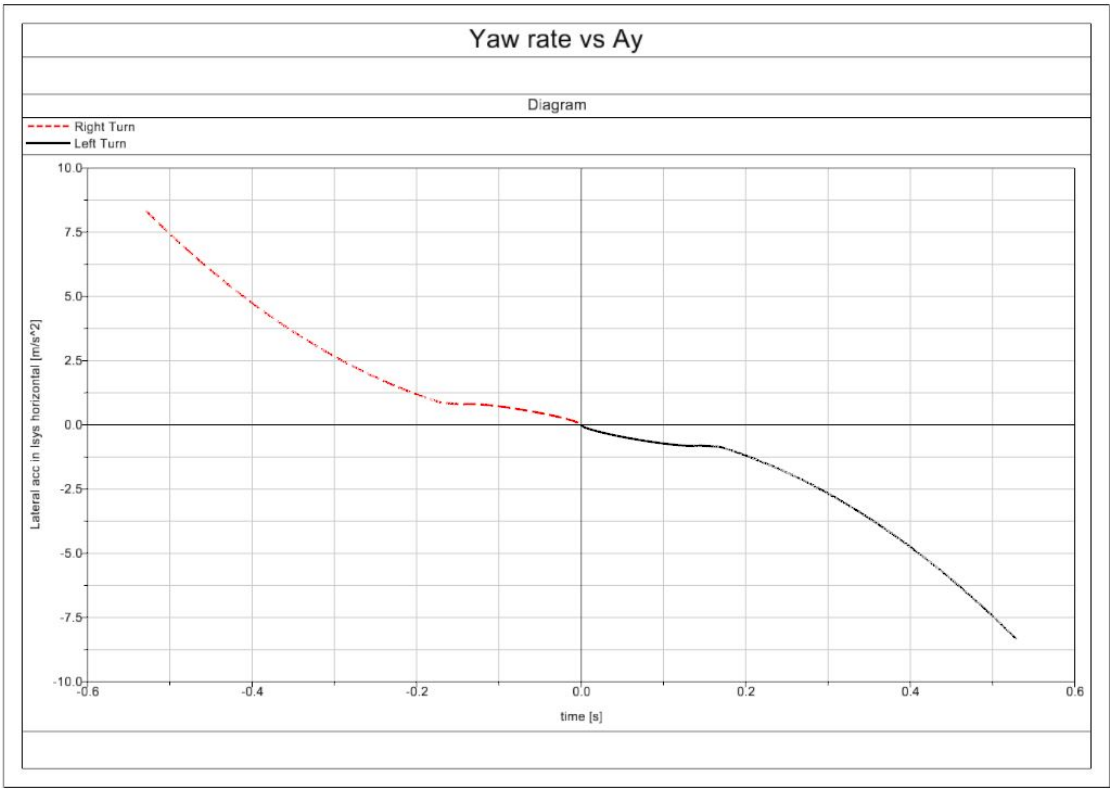

Figure 46 Yaw Rate vs. Lateral Acceleration [g] From Constant Radius Loadcase

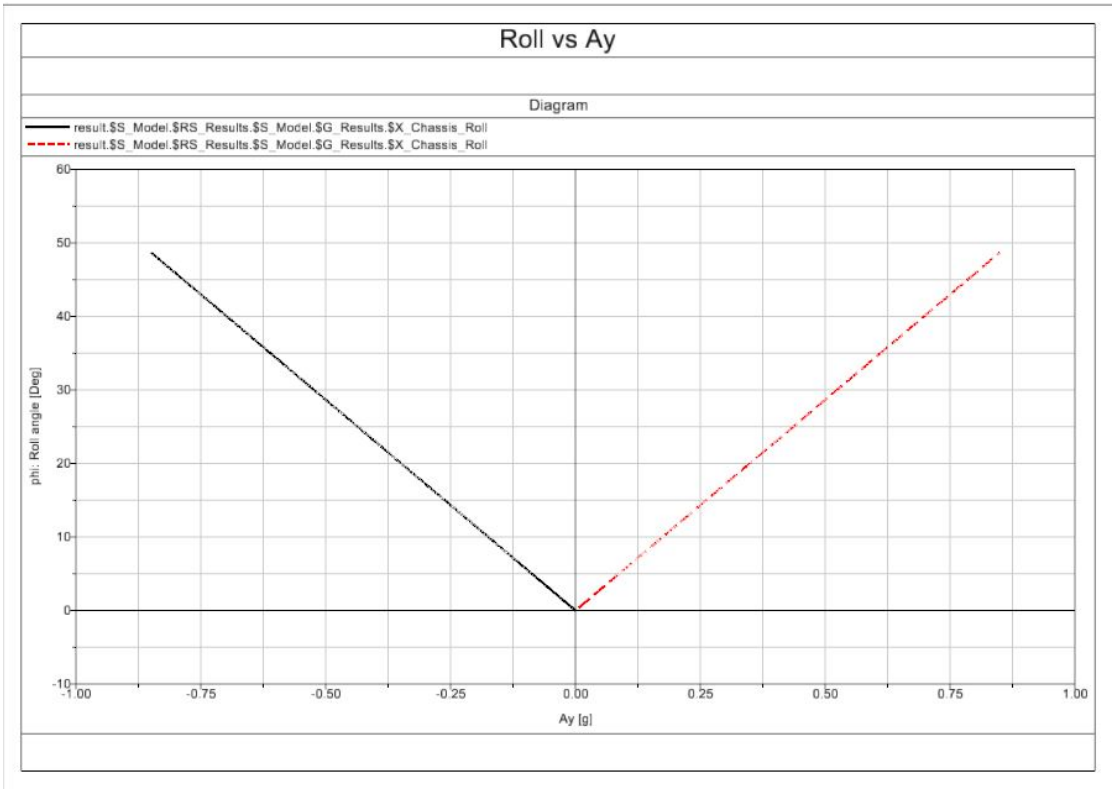

Figure 47 Roll vs. Lateral Acceleration [g] From Constant Radius Loadcase

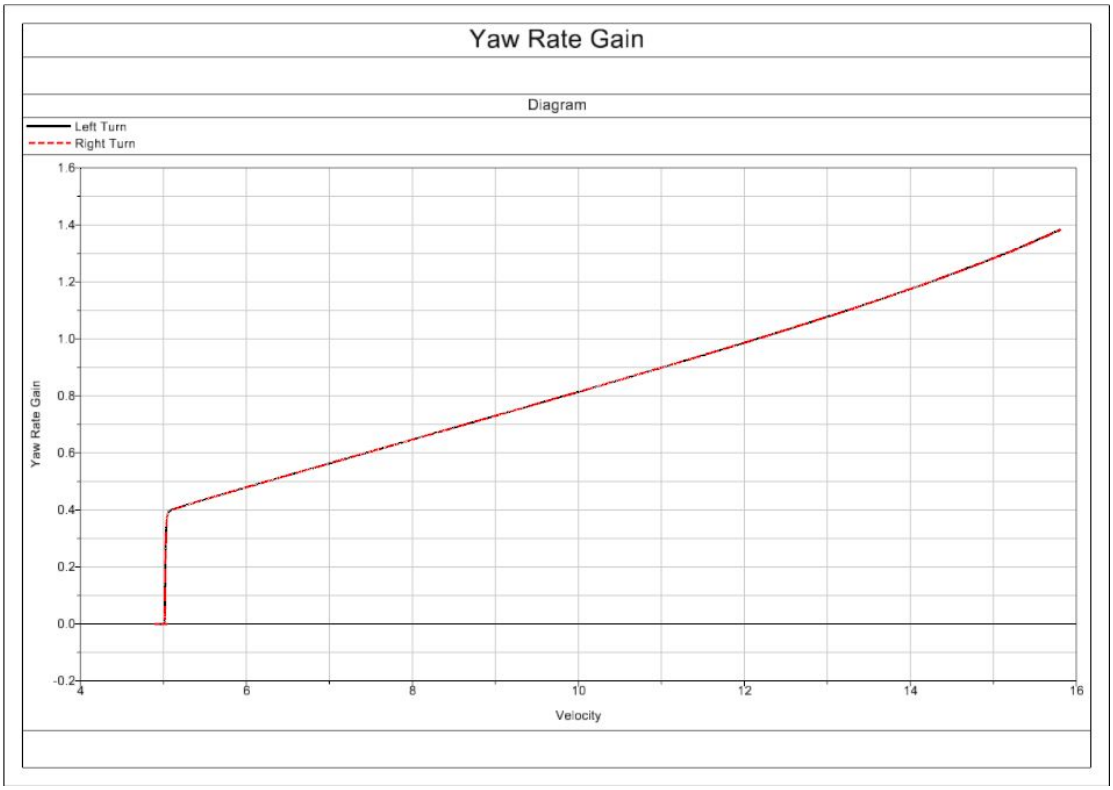

Figure 48 Yaw Rate Gain

3.5 Desired Body Slip Angle , Body Slip Angle Estimation and Low Coefficient of Friction Modelling

In order to determine the benefit of slip angle controlled ESC and the benefit of real time slip angle sensing, a desired body slip angle and an estimated body slip angle will need to be determined.

3.5.1 Desired Body Slip Angle

The desired body slip angle has been calculated using Equation 40. The desired body slip angle is calculated based upon the vehicle longitudinal velocity, the steering wheel angle and vehicle parameters such as wheelbase and cornering stiffness. The cornering stiffness is determined from the lateral force vs slip angle plot as seen in Figure 47, for the static front and rear vertical loads.

Equation 40 Desired Body Slip Angle (Rajamani, 2006)

3.5.2 Body Slip Angle Estimation and Low Coefficient of Friction Modelling

The body slip angle is estimated using the method proposed by Hac & Bedner (Hac & Bedner, 2007), which has been previously outlined. The method proposed by Hac & Bedner is based on Equation 41 and Equation 42.

Equation 41 Lateral Velocity Estimation by Pseudo Kinematic Integration (Hac & Bedner, 2007)

Equation 42 Estimated Body Slip Angle from the Estimated Lateral and Longitudinal Velocity by Pseudo Integration (Hac & Bedner, 2007)

Low Coefficient of Friction Modelling and Results

A key feature of this estimation technique is the use of a look up tables in order to estimate the lateral force at the front and rear axle. The lookup tables consist of empirical data of lateral force vs tyre slip angle for both high and low road tyre friction coefficients. Hac & Bedner acquire this data from a steady state test, with this in mind the pre defined constant radius test was used.

In order to acquire the data required for the simulation both low coefficient and high coefficient of friction simulations needed to be carried out, in this case the coefficients of friction were 0.1 and 1 respectively. In order to achieve the different coefficients of friction the tyre road friction variable was modified in the loadcase. The variation of this parameter has a significant effect on tyre behaviour this can be seen particularly when looking at Figure 49. The red data series shoes the Longitudinal Force vs Longitudinal Slip for varying normal force for a tyre with the low friction coefficient, whereas the blue data series shows the same but for a tyre with the high friction coefficient. It is immediately clear to see that when the road tyre friction is low the achievable longitudinal force is significantly low; this would have a significant affect on the vehicle's longitudinal dynamics. It is interesting to note that with both coefficients of friction, as the normal load increases, the peak longitudinal force increases, but on average for a given normal load the peak longitudinal force is ten times lower when the road tyre friction coefficient is low.

Figure 49 Coefficient of Friction Comparison of Lateral Force vs Slip Angle

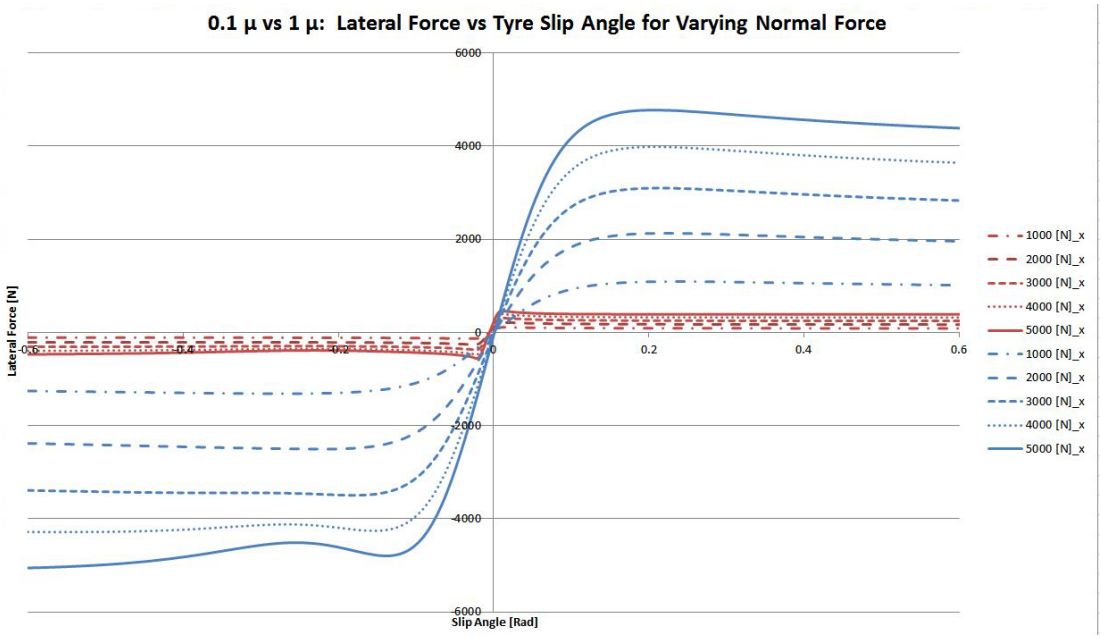

The same trend can be seen when looking at Figure 50 which shows lateral force vs slip angle for varying normal loads. As this particular investigation focuses on lateral dynamics, Figure 49 is of high importance as it fundamentally shows how the lateral vehicle behaviour changes due to a reduction in the road tyre friction coefficient. Figure 49 shows that there is a significant reduction in the tyre's ability to create lateral force, which will have a significant effect on the vehicle's ability to change path.

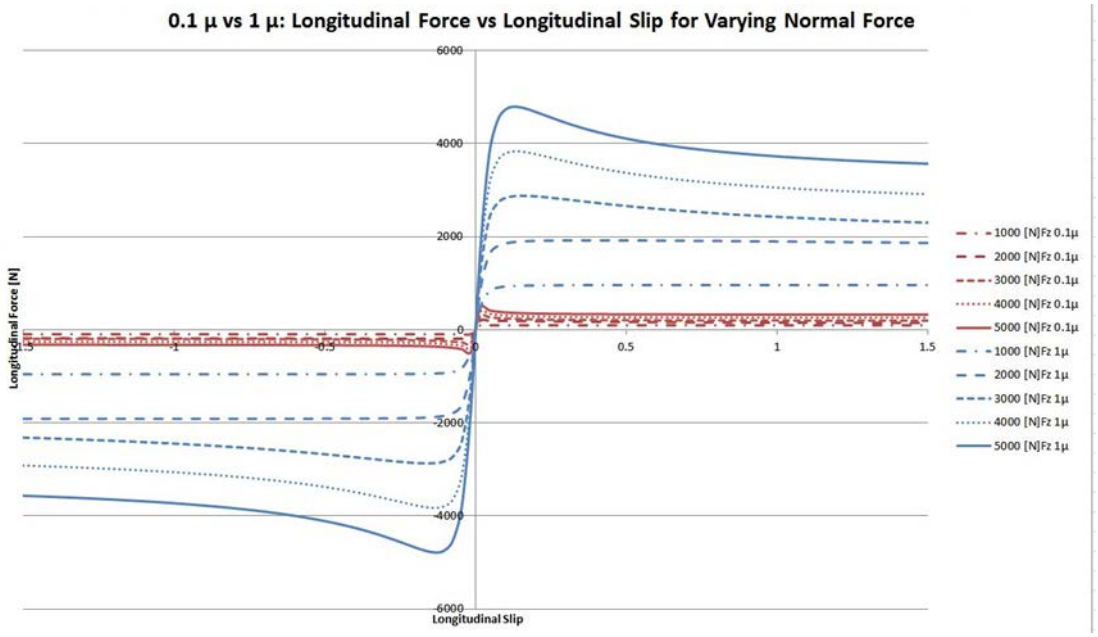

Figure 50 Coefficient of Friction Comparison of Longitudinal Force vs Longitudinal Slip

In order to get the lateral axle force vs slip angle data required for the body slip angle estimator the constant radius loadcase simulation was carried out, for both friction coefficient conditions. As previously mentioned in the constant radius loadcase the vehicle is slowly accelerated around a 30m radius, in this case this is continued, if possible, until 0.85g is achieved. As expected the constant radius results show that when the coefficient of friction is low the vehicle is unable to achieve 0.85g as seen in

Figure 51. Fundamentally this is because when the coefficient of friction is low, the peak lateral force is reached quickly at low tyre slip angles, as the tyre slip angle is increasing the lateral force isn't increasing (as seen in Figure 49) . The required lateral force to achieve 0.85g is unattainable; in this case, the maximum lateral acceleration achieved due to the low coefficient friction is ~ 0.1g. It is interesting to note when looking at

Figure 51, up to ~0.1g there is no difference in the vehicle's lateral acceleration response between the two simulations, even though the coefficient of friction is significantly different. This further highlights the need for intelligent vehicle safety systems, as in this particular situation the driver would be unaware that they were about to lose control of the vehicle.

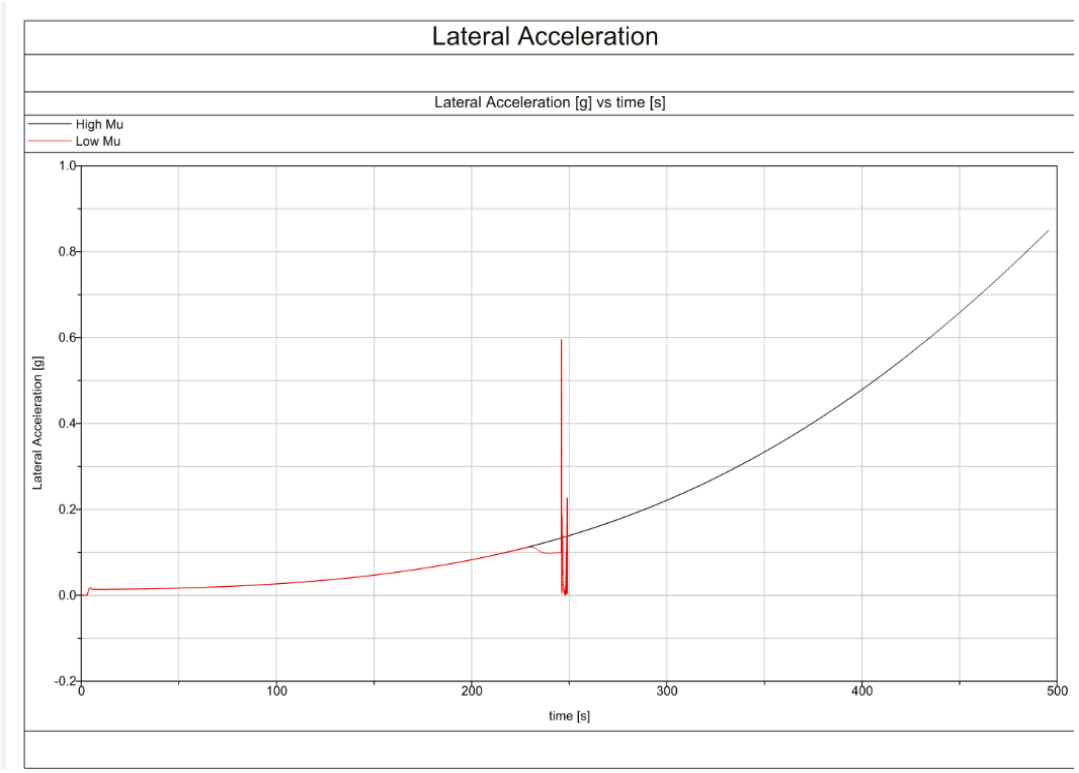

Figure 51 Lateral Acceleration Comparison of a Constant Radius Loadcase high and low coefficient of friction

3.6 ESC Control System Modelling

In order to carryout, the investigation an ESC control system was created in SIMPACK. A control system is a system designed to command, direct or regulate itself or another system (DiStefano III, et al., 1990). The control system created for the investigation is a PI (Proportional Integral) controller. This controller method was used fundamentally, because it is a widely adopted controller method for a variety of applications (due to its simplicity) and it could be easily implemented into SIMPACK.

3.6.1 Proportional Integral Controller

A PI controller is a closed loop controller. The behaviour of a closed loop controller is dependant on its output, i.e. the output of the controller has a direct effect on the input of the controller. Simplistically a PI controller uses an error determined by the difference between a particular output from the plant and the set point. The error then goes through both the proportional path and the integral path. In the proportional path of the controller, the error is simply multiplied by a gain; therefore, if the error is large the output from the proportional path is large, if the error is zero so is the output from the path, the sign of the output from the proportional path also stays consistent with the error. In the integral path of the controller, the integral of the error is multiplied by a gain. The integral of the error summates the error as it changes through time, therefore constant errors (even very small consistent errors) can affect the controller output. The summation of the outputs from the proportional path and the integral path of the controller form the controller's output, which is fed into the Plant. The output of plant, (after it has been affected by the controller) is then fed back into the controller. Figure 54 shows the generic setup of a PI controller.

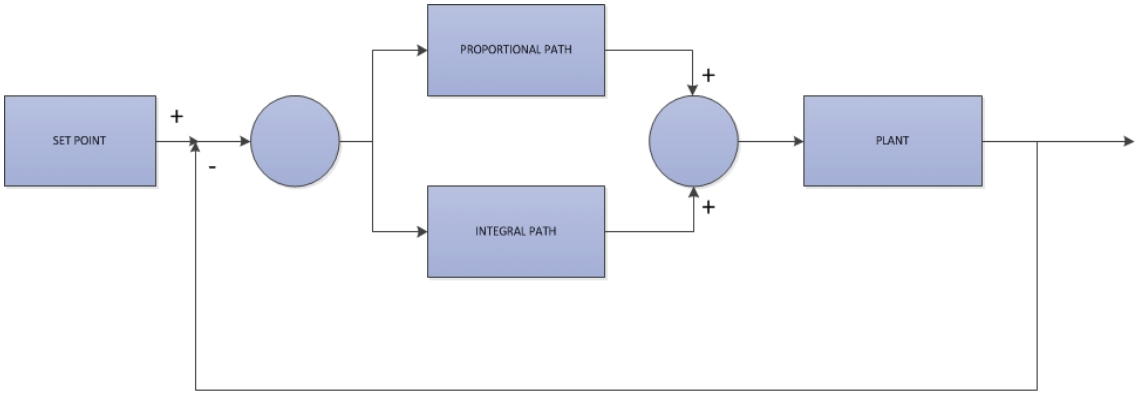

Figure 54 Generic PI Controller

3.6.2 Proportional Integral Controller for Electronic Stability Control

In order to create a PI controller that can be used as an electronic stability control system the various aspects of a PI controller need to be determined. Firstly, the set point needs to determined, in this case the ESC system is trying to control the vehicle's body slip angle based upon the vehicle's current body slip angle and the vehicle's desired body slip angle. The set point is the vehicle's desired body slip angle which is determined by an equation based on the vehicle's current behaviour as seen in 3.5.1 Desired Body Slip Angle.

Next, the proportional and integral control paths need to be implemented. SIMPACK has a built-in PID (Proportional Integral Differential) control element that can be also be used to create the variations of a PID, such as a PI controller. The PI control element simply requires an error input and two gain factors, one for each path. The error is determined as the difference between the actual (measured) body slip angle and the desired body slip angle. In order to determine the gain factors, the control element and plant need to be implemented. The plant in this ESC system is implemented as brake force applied at each wheel, the braking force is the summation of the proportional and integral path. Simple control logic based on TANH of the vehicle's yaw rate is used to determine the vehicle's direction, which is used to determine which of the wheels to brake to control the vehicle's body slip angle. The braking is set up in pairs, the front left and rear right wheels are a pair, and the front right and rear left are the other pair, i.e. if the vehicle's direction is positive then the front right and the rear left wheel are braked. A breakdown of the system can be seen in Figure 55.

The gains for the proportional and integral path were tuned by the trial and error method once the system became functional. In this particular case the gains were tuned using the sine with dwell loadcase, the gains were tuned (by increasing and decreasing their value) until an optimum controller behaviour was obtained, in this case the vehicle's actual body slip angle quickly matched the vehicle's desired body slip angle (i.e. the error was zero, or the error became zero after a short period of time).

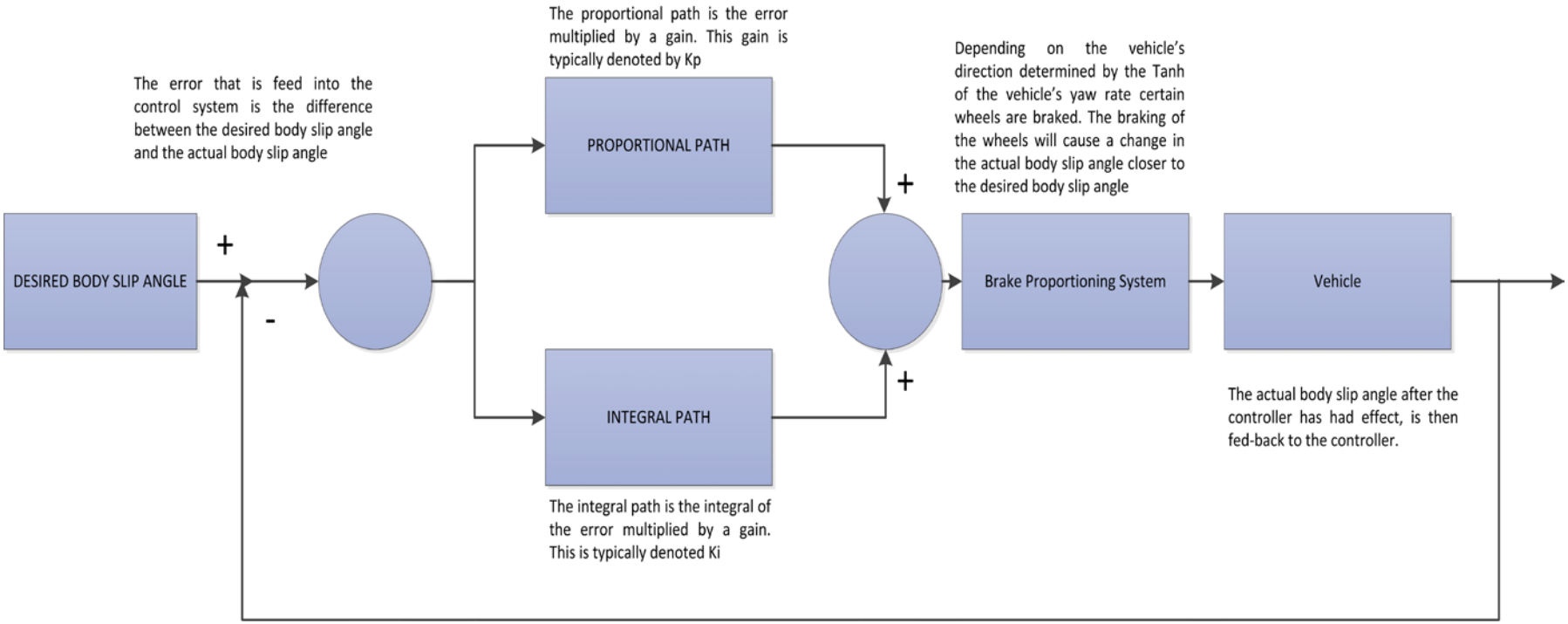

Figure 55 PI Controller for ESC Simulation

4.0 RESULTS AND ANALYSIS

The simulation sets out to determine if a calculated desired body slip angle could be used to for electronic stability control. Current systems typically use desired yaw rate, but the use of body slip angle control could prove beneficial. The investigation process sets out to:

- Determine if the ESC system, desired body slip angle and estimated body slip angle are functioning correctly during with the constant radius test.

- Determine if the ESC system, desired body slip angle and estimated body slip angle are functioning correctly during the sine with dwell test

4.1 Constant Radius Results and Analysis

An initial constant radius test was run up to 0.85g with ESC switched off in order to determine if the estimated, desired and measured body slip angles correlated. Initial constant radius results seen in Figure 52 showed that the measured body slip angle and estimated body slip angle correlated well but there was a significant discrepancy seen in the desired body slip angle. It was expected that the desired body slip angle would be similar to the measured body slip angle until about ~0.5g when the tyres began to behave non-linearly, whereas the results showed discrepancies at lateral accelerations as low as 0.1g. As this was not expected, further investigation was carried out. On reflection of the initial vehicle characterisation test, it was clear to see that during the constant radius test there was a significant change in the tyre vertical forces as seen in the lateral load transfer plots seen in Figure 44 and Figure 45. The tyre vertical forces have an effect on the lateral force vs. slip angle plots as seen in Figure 43, therefore the tyre vertical forces have an effect on the tyre cornering stiffness. It was assumed that this discrepancy was due to the use of static cornering stiffness values for the desired body slip angle calculation. With this in mind a lookup table of cornering stiffness vs. vertical load, was generated from the tyre curves so that varying cornering stiffness could be used to determine the desired body slip angle. This approach yielded the results as initially expected as seen in Figure 53.

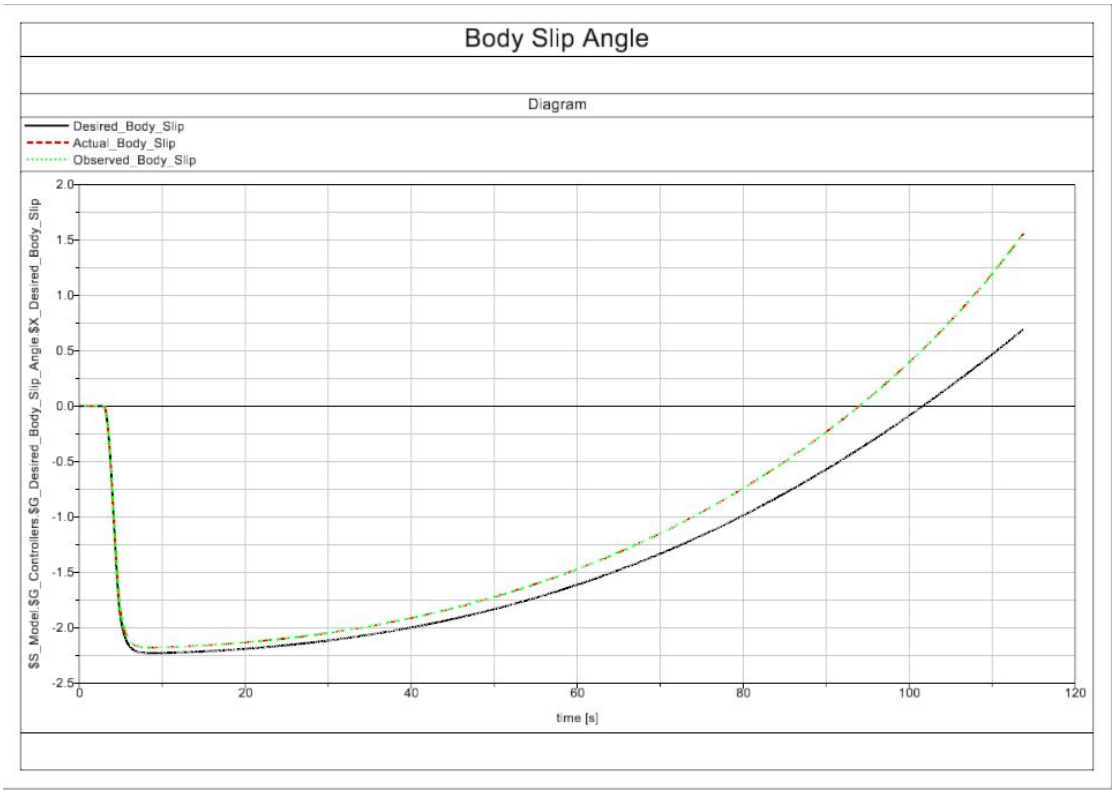

Figure 52 Initial Body Slip Angle Results from the Constant Radius Loadcase

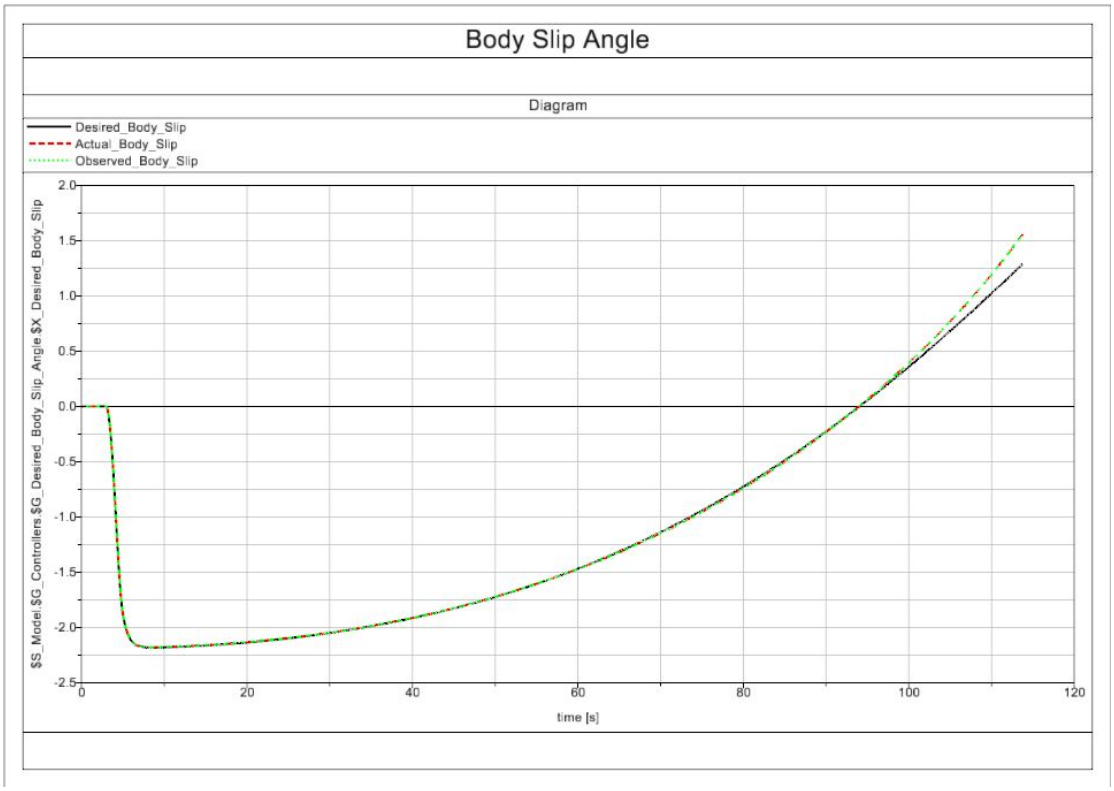

Figure 53 Body Slip Angle Results with Varying Cornering Stiffness included from the Constant Radius Loadcase

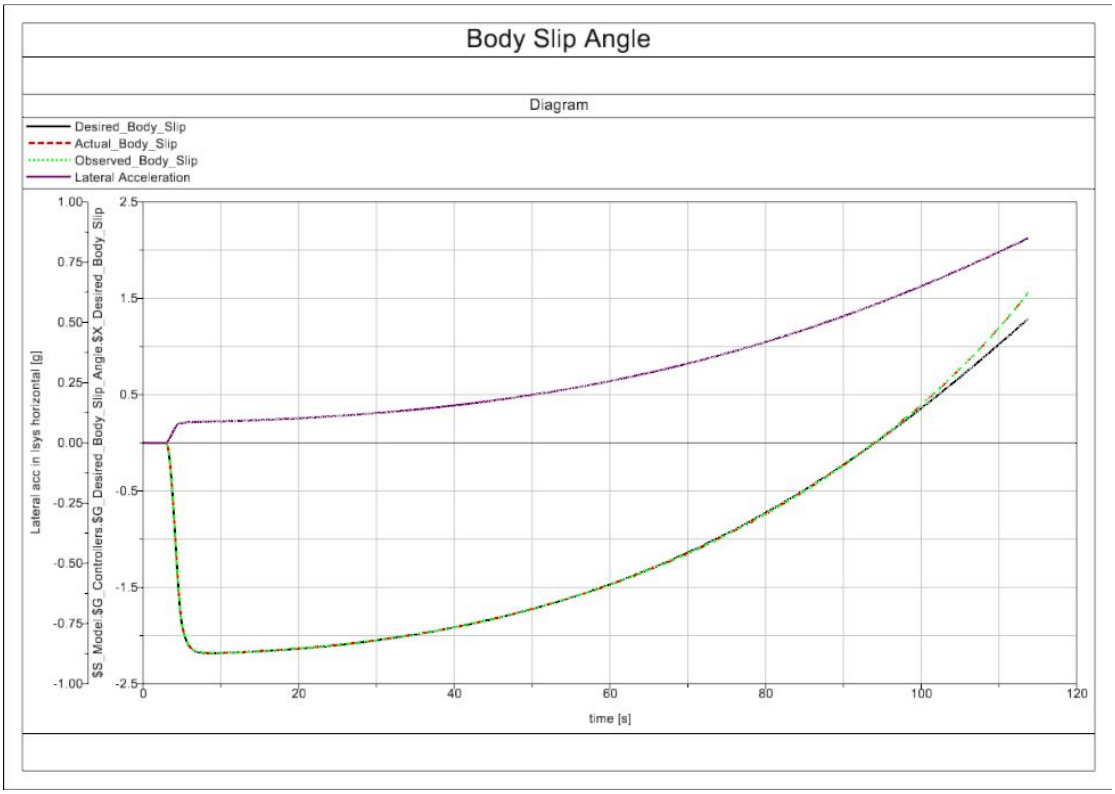

Figure 54 Body Slip Angle and Lateral Acceleration Results with Varying Cornering Stiffness included, from the Constant Radius Loadcase

Figure 54 shows, as expected, the desired body slip angle begins to vary from the measured and estimated body slip angle at ~0.6g as the non-linearity of the tyres begin to take effect. As it is clear that the desired, measured and estimated body slip angles are behaving as expected, a third constant radius simulation is run, to determine if the ESC system is working effectively. Figure 55 shows that the ESC system based on desired body slip angle is successful in controlling the body slip angle up to 0.85g.

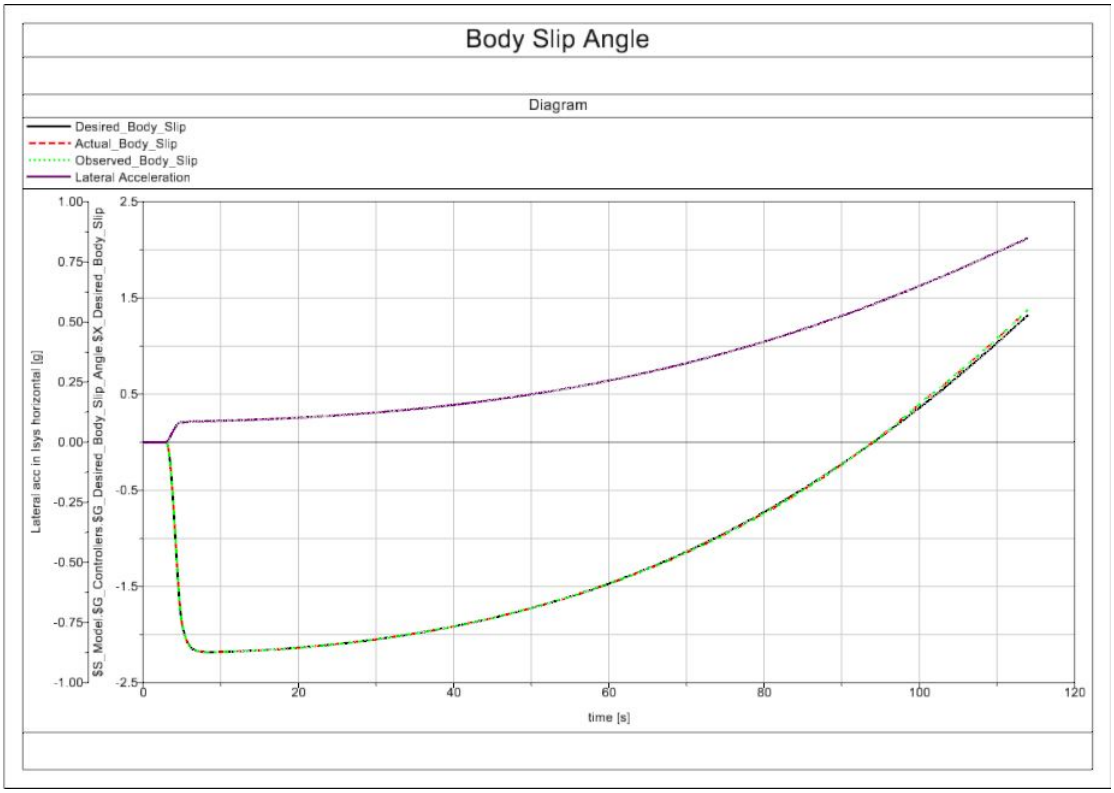

Figure 55 Body Slip Angle and Lateral Acceleration Results with Varying Cornering Stiffness Included, and ESC System Enabled from Constant Radius Loadcase

4.2 Sine with Dwell Results

As previously mentioned as part of the sine with dwell protocol an initial pre test is carried out to determine the steering wheel angle amplitude 'A' that will be used for the main part of the test. The amplitude "A", which is the steering wheel angle that produces a steady state lateral acceleration 0.3g, is 0.55 radians for the model. Once the amplitude "A" was determined, an initial sine with dwell test was carried out at 1A. Figure 56 shows the desired, measured, and estimated body slip angle for the sine with dwell test carried out at 1A, it is clear to see that the measured and estimated body slip angle correlate, but the desired body slip angle seems to been more responsive than measured and estimated body slip angle. As this is not expected due to the exceptional correlation seen with the constant radius test further investigation was carried out.

The further investigation showed that overall the desired body slip angle equation was not ideal for transient events. Further analysis showed that simply using yaw rate as a gain could improve the desired body slip angle. Unfortunately, due to limitations in time further investigation into improving the desired body slip angle was not carried out.

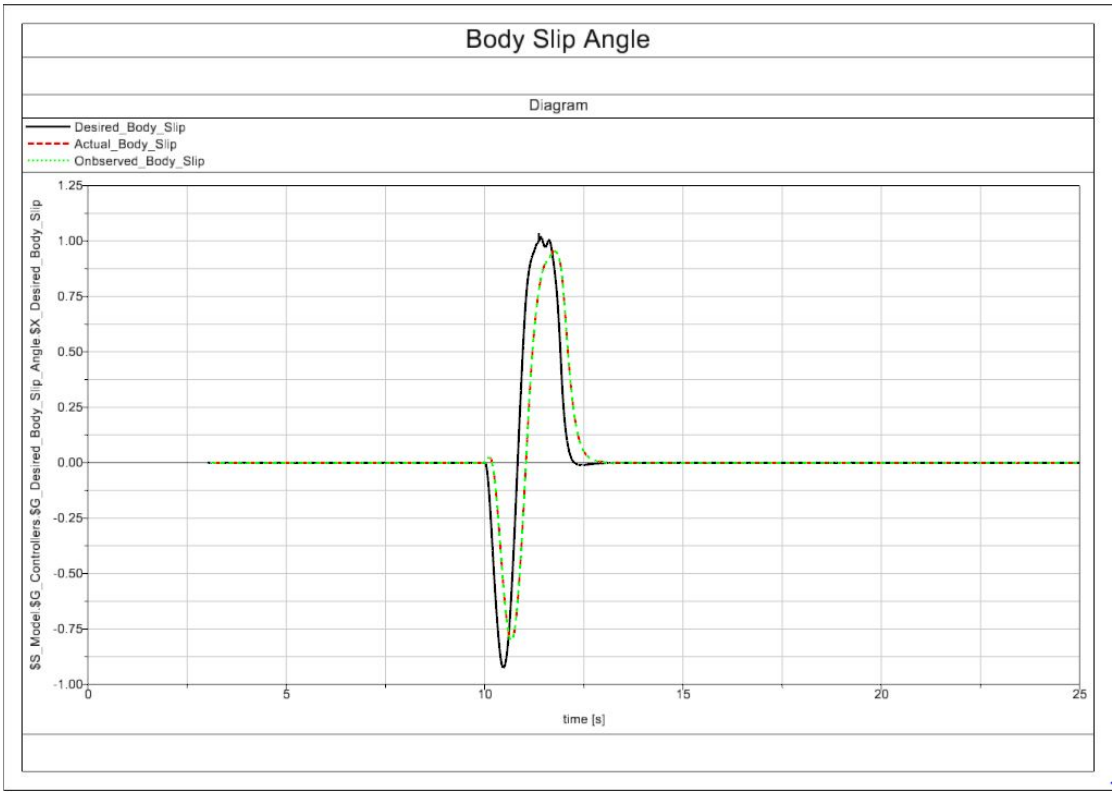

Figure 56 Desired Body Slip Angle, Actual Body Slip Angle and Observed Body Slip Angle for the Sine with Dwell Loadcase at Amplitude "A"

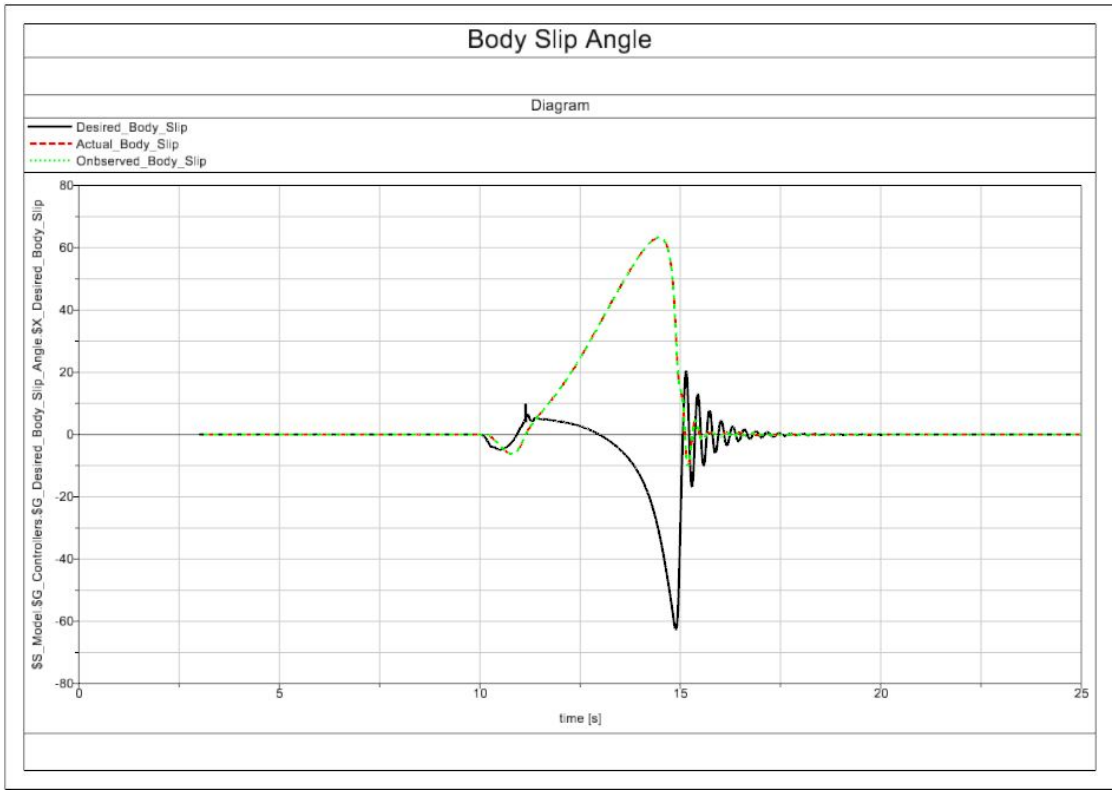

Figure 57 Desired Body Slip Angle, Actual Body Slip Angle and Observed Body Slip Angle for the Sine with Dwell Loadcase at Amplitude "5A" with ESC System Inactive

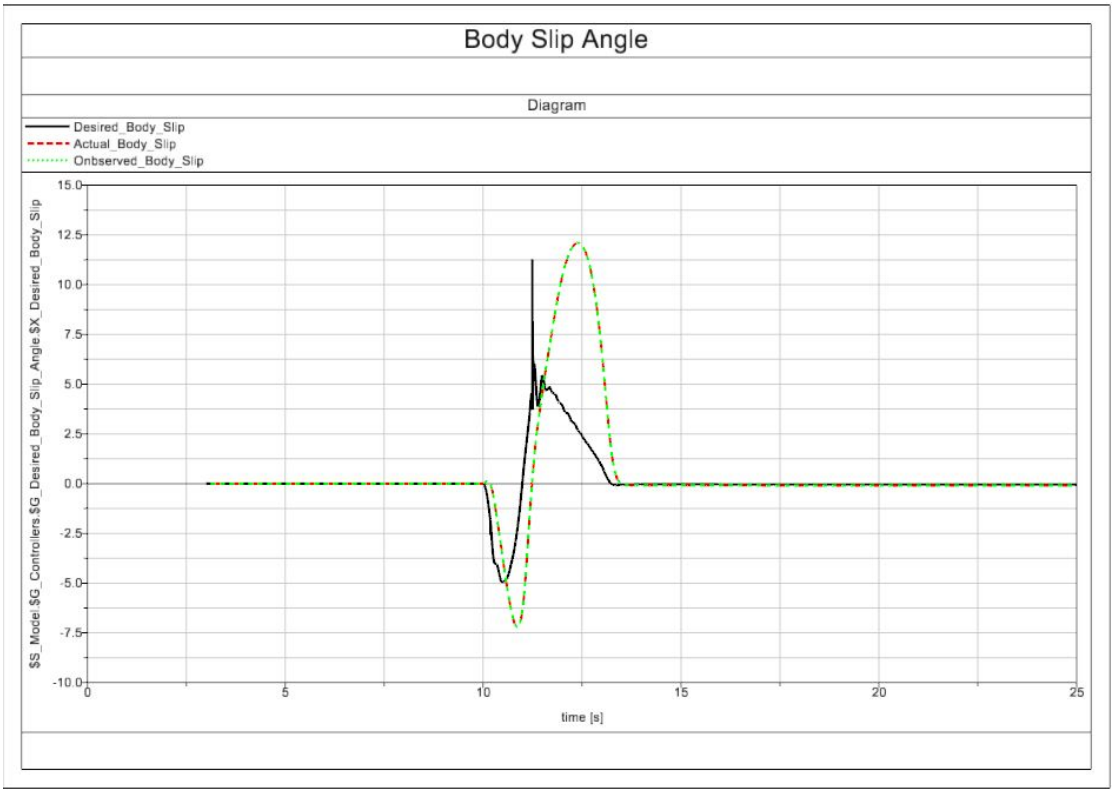

Figure 58 Desired Body Slip Angle, Actual Body Slip Angle, Observed Body Slip Angle for the Sine With Dwell Loadcase at Amplitude " 5A" with ESC System Active

It is worth noting that even though the desired body slip angle did show this error, it could still be successfully used to with the ESC system, to control the body slip angle and pass the sine with dwell test, this can be seen when comparing Figure 57 and Figure 58. Figure 57 shows a sine with dwell manoeuvre with amplitude 5A; it is clear to see that the body slip angle is uncontrolled as it peaks at about 60 degrees. It is also interesting to note the desired body slip angle produces erroneous results, but this may be due to the vehicle spinning. Figure 58 shows the same scenario with ESC switched on, even though the desired body slip angle is offset, the ESC system manages to control the body slip angle and the sine with dwell manoeuvre is achieved. This suggests that further development in both the ESC system and the desired body slip angle could produce a desirable body slip angle target ESC system.

4.3 Body Slip Angle Vs Yaw Rate Results in Low Friction Conditions

In order to determine the effectiveness of using body slip angle or yaw rate as an indicator of a vehicle's current behaviour, simulations based on the previously defined loadcases are carried out. The simulations involved reducing the road tyre friction coefficient from 1 to 0.5 in 0.1 intervals for both loadcases. Figure 59 and Figure 62show the yaw rate and body slip angle for varying road tyre coefficients respectively for the constant radius loadcase.

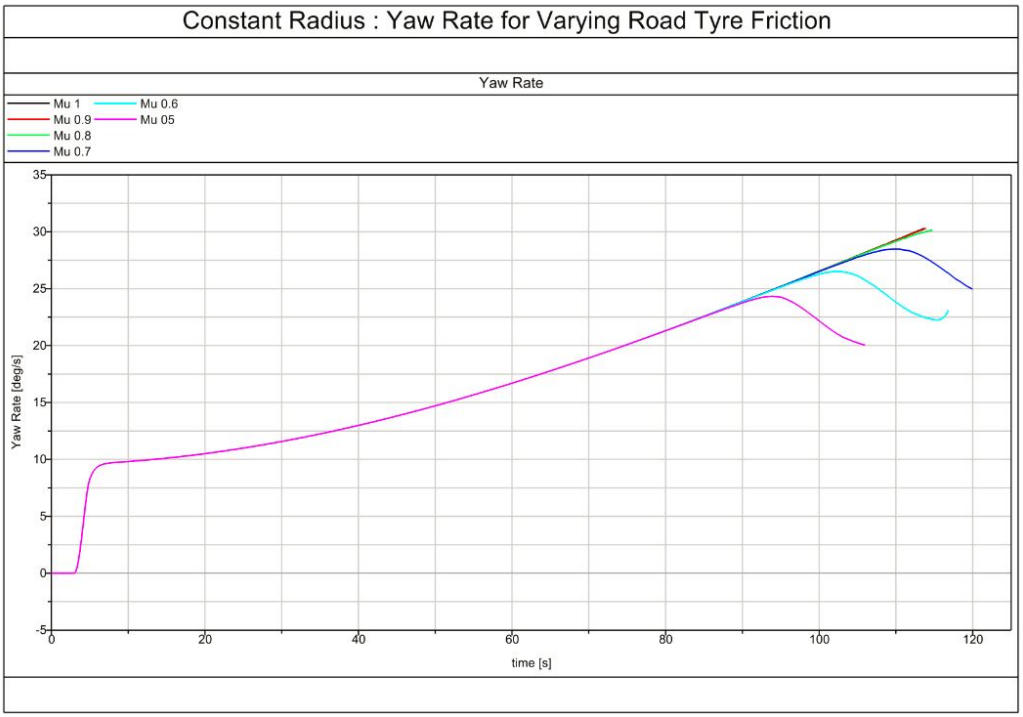

Figure 59 Constant Radius: Yaw Rate for Varying Road Tyre Friction

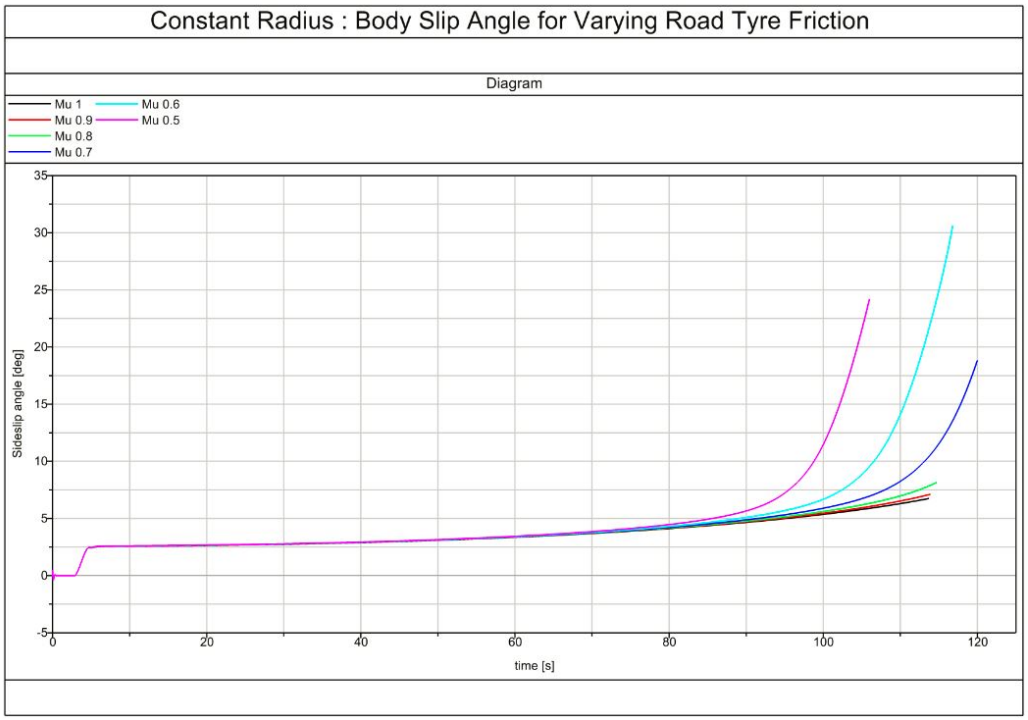

Figure 60 Constant Radius: Body Slip Angle for Varying Road Tyre Friction

It is clear to see when looking at both figures that the vehicle behaviour significantly changes when the road tyre friction coefficient decreases past 0.7, this is because when the road tyre friction coefficient decreases the lateral force achievable by the tyres is decreased. In this particular instance, the tyres are no longer able to create the lateral force required for the vehicle to maintain the constant radius. As the road tyre, friction coefficient decreases both the yaw rate and body slip angle show a change in vehicle behaviour, as expected the lower the coefficient of friction the sooner the change in vehicle behaviour. When evaluating the effectiveness of using either body slip angle or yaw rate to determine vehicle behaviour, it is clear to see that in this particular situation the yaw rate would be inadequate, as the yaw rate actually decreases when the vehicle is behaving undesirably, so a control system based on a yaw rate threshold would not engage. On the other hand, the body slip angle increases at a comparatively high rate quickly exceeding normal body slip angles with the vehicle behaviour is undesirable, therefore in this particular situation using body slip angle, as an indicator of vehicle behaviour is ideal, as a control system would quickly engage when the vehicle behaviour is undesirable.

As the constant radius loadcase is a steady state test the same simulation was carried out with the sine with dwell loadcase, which is a transient test, to further validate the use of body slip angle as an indicator of vehicle behaviour. The sine with dwell tests are at relatively high amplitude, the steering angle amplitude is four times more than what is required to reach 0.3g (i.e. 4A, as previously defined). At this steering wheel amplitude, the yaw rate of the vehicle will be high, but the vehicle is able to complete the manoeuvre successfully with a high coefficient of friction. Figure 61 and Figure 62 show the yaw rate and body slip angle for varying coefficients of friction respectively. It is clear to see that both the yaw rate and body slip angle for the sine with dwell loadcase shows a similar trend as the yaw rate and body slip angle for the constant radius loadcase. When looking at the yaw rate it is clear to see that as the coefficient of friction decreases, and the vehicle's behaviour becomes undesirable, the peak yaw rate of the vehicle decreases, except for when the vehicle fails the manoeuvre with a 0.5 friction coefficient. When the vehicle fails the manoeuvre, the yaw rate rapidly increases. In contrast, the body slip angle increases as the coefficient of friction decreases and when the vehicle fails the manoeuvre, the body slip angle is already significantly high, providing a better indication of the vehicle behaviour sooner.

It is clear to see that based on the varying coefficient of friction results; the body slip angle provides a better indication of the vehicle's current behaviour when the coefficient of friction is low. It is worth noting that for both simulations both yaw rate and body slip angle are an accurate representation of the vehicle behaviour when the coefficient of friction is high, but the body slip angle shows a more gradual change in vehicle behaviour, making it easier to identify when the vehicle behaviour is going to become undesirable.

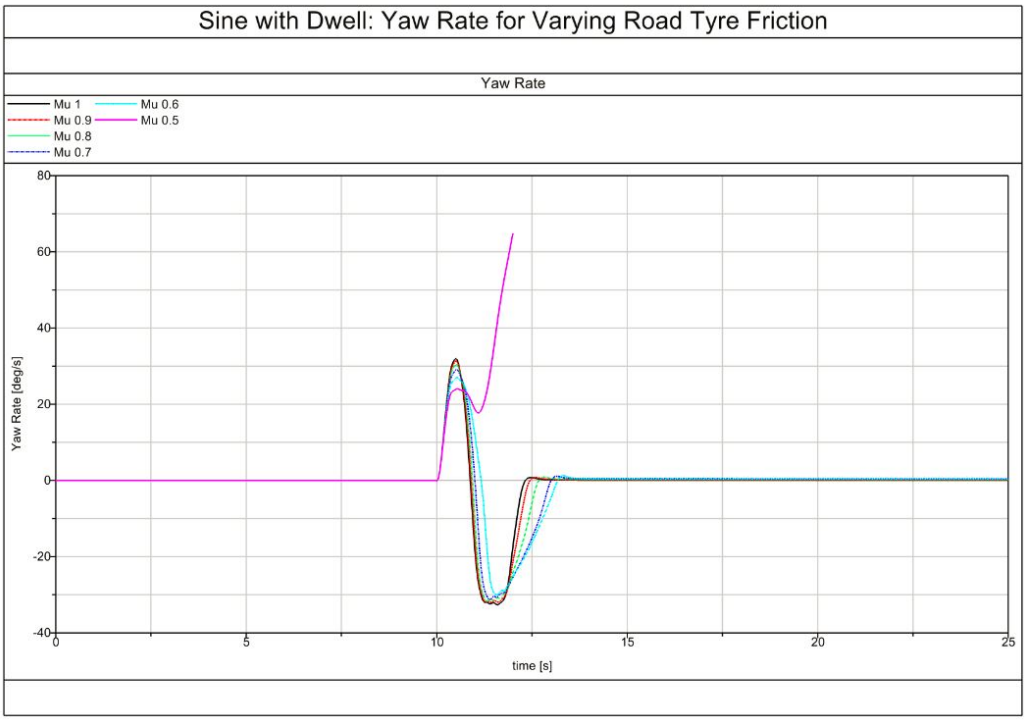

Figure 61 Sine with Dwell: Yaw Rate for Varying Road Tyre Friction

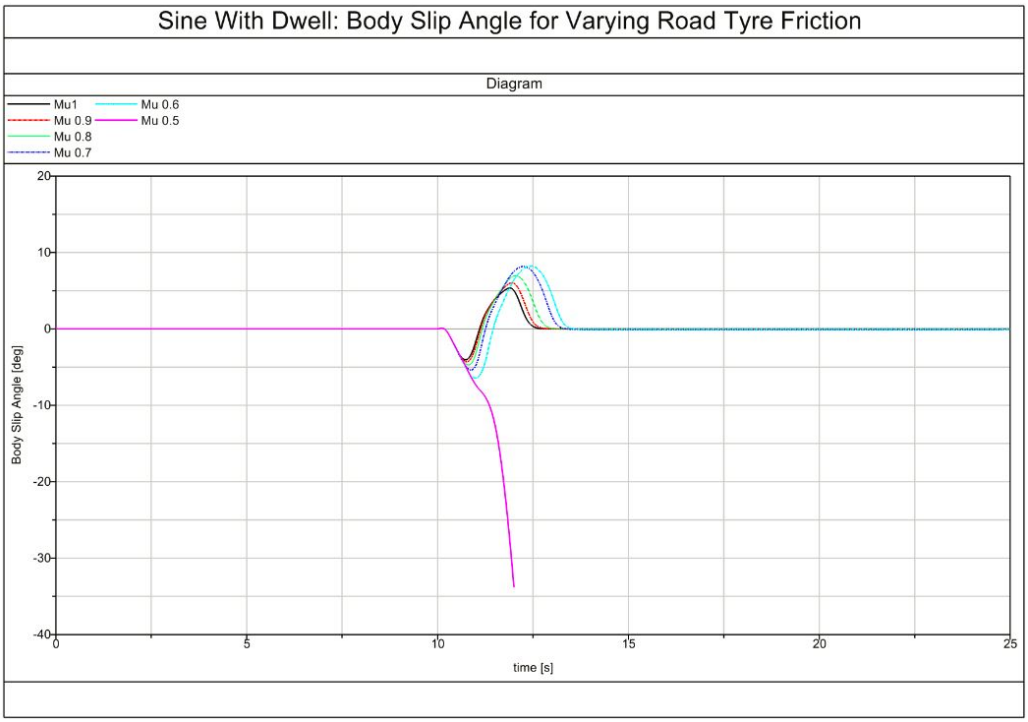

Figure 62 Sine with Dwell: Body Slip Angle for Varying Road Tyre Friction

5.0 CONCLUSION

Literature has shown that vehicle safety systems could be enhanced by the use of live slip angle data, as current estimation methods are not robust enough for control purposes. It is also seen that a key task of ESC, is body slip angle control, but due to lack of robust estimation, the control system aims to control the body slip angle, by yaw rate control.

Various viable technologies for body slip angle sensing have been researched, all with their own advantages and disadvantages, for example INS/GPS are affordable and less prone to noise when compared to optical sensors, but optical sensors are highly accurate and immune to signal loss. Research also showed that laser Doppler velocity sensors could be an accurate affordable body slip angle sensor, based on this a laser doppler velocity sensor based ESC system has been proposed. The proposed ESC system not only allows for robust body slip angle measurement, but can also provide vehicle information that helps determine if a vehicle is understeering or oversteering.

The desired body slip angle requires significant investigation and development. Fundamentally the equation used to determine the desired body slip angle only works for steady state situations, this can clearly be seen as the equation does not include yaw rate. The simulation results show that ESC systems that target a desired body slip angle are effective, even though the desired body slip angle is not completely accurate in the dynamic situations. The body slip angle based ESC system successfully reduces the body slip angle, which allows for the sine with dwell manoeuvre to be successfully completed. The key conclusion can be seen when looking at the low coefficient of friction simulations, which show the benefit of body slip angle sensing. It is clear to see from the simulation results that when the road tyre friction coefficient is low, the yaw rate does not successfully capture the instability of the vehicle, but the body slip angle does. It is interesting to note that traditional ESC systems that estimate body slip angle would also not be able to capture the vehicle instability due to the cascade controller set up, where the measured yaw rate verifies the body slip angle. In this particular situation if the body slip angle estimation was accurate, the controller may determine the body slip angle incorrect because the body slip angle is high and the yaw rate is low, therefore the controller may not instigate any change in vehicle behaviour, this highlights a key limitation of current ESC systems.

Overall, it is clear to see that acquiring real time body slip angle could prove beneficial to automobiles as current ESC systems aim to control the body slip angle based on body slip

angle estimations. The body slip angle estimations are not always accurate, particularly on low coefficient of frictions situations and therefore the effectiveness of an ESC system when the coefficient of friction is low is compromised. Many methods of acquiring live body slip angle have been investigated, it is clear to see that Laser doppler velocity sensors are the most suitable technology for real time body slip angle sensing when compared to GPS, optical sensors and radar doppler velocity sensors.

6.0 RECOMMENDATIONS FOR FURTHER STUDY

Whilst completing the aims of the investigation and satisfying the research question, it is clear that there are certain areas of research that could benefit from further investigation these include:

- Enhancement of the desired body slip angle with the inclusion of yaw rate
    - Although the investigation has shown that targeting a desired body slip angle is a successful approach in creating an ESC system, further research is required in order to determine the desired body slip angle, as the approach used in the investigation is not suitable in dynamic situations. A suitable approach would be to find a desired body slip angle equation with the inclusion of yaw rate, which can be determined by the proposed laser Doppler velocity sensors.

- Further determination of the benefits of real time slip angle sensing, by using body slip angle to determine the coefficient of friction and using it as an input into the control system.
    - The investigation clearly shows that when the coefficient of friction is low, the vehicle's body slip angle is a better indicator to determine if the vehicle's behaviour is undesirable, but further research can be carried out to determine if the body slip angle sensors could provide information on the coefficient of friction. If the body slip angle sensors could be used to determine the coefficient of friction of the road surface, different vehicle control techniques (such as steering angle intervention) could be utilised when traditional brake modulation would not suffice.

- Determination of how body slip angle can be used in conjunction with steer by wire and torque vectoring

- The investigation only focuses on traditional vehicle control methods such brake modulation, but further research into the other vehicle control strategies such as steering angle intervention via steer by wire and torque vectoring could prove beneficial for electronic stability control. The investigation into other vehicle control methods could prove extremely beneficial if the body slip angle sensors can be utilised to determine the coefficient of friction for the road surface.

Overall the investigation carried out would provide a suitable basis for researching the areas of further study. The investigation can be used to emphasise the need for real time slip angle sensing, the limitations of body slip angle estimation, the potential of using real time body slip angle for ESC and the use of doppler velocity sensors for real time slip angle sensing

References

Baba, K. et al., 1979. *Doppler Radar Speed Sensor for Anti-Skid Control System,* s.l.: Society of Automotive Engineers Inc.

Beiker, S. A., Gaubatz, K. H., Gerdes, J. C. & Rock, K. L., 2006. *GPS Augmented Vehicle Dynamics Control,* Michigan: SAE International.

Bevly, D. M., Daily, R. & Travis, W., 2006. *Estimation of Critical Tire Parameters Using GPS based Sideslip Measurements,* Michigan: SAE International.

Blundell, M. & Harty, D., 2004. *The Multibody Approach to Vehicle Dynamics.* 1st ed. Oxford: Elsevier.

Corrsys Datron, n.d. *The Physical Operating Principle of CORREVIT Non-Contact Optical Sensors,* s.l.: s.n.

DiStefano III, J. J., Stubberud, A. & Williams, I. J., 1990. *Feedback and Control Systems.* 2nd Edition ed. Irvine(Los Angeles): Mc Graw Hill.

Ditchi , T., Hole, S., Corbrion, C. & Lewiner, J., 2002. *On Board Doppler Sensor for Absolute Speed Measurement in Automotive Applications,* Michigan: SAE International.

Erdogan, G., Sanghyun, H., Borrelli, F. & Hedrick, K., 2011. *Tire Sensors for the Measurement of Slip Angle and Friction Coefficient and Their Use in Stability Control Systems ,* Berkeley: SAE International.

Euro NCAP, 2011. *The Dynamic Test Of Car Electronic Stability Control (ESC) Systems Protocol,* s.l.: Euro NCAP.

Euro NCAP, 2015. *Electronic Stability Control.* [Online]
Available at: http://www.euroncap.com/en/vehicle-safety/the-ratings-explained/safety-assist/esc/
[Accessed 12 03 2015].

Galmiche, B., Halter , F. & Foucher, F., 2013. *Experimental Investigations for Turbulent Premixed Flame Analysis,* United States: SAE International.

Gao, X. & Yu, Z., 2010. *Nonlinear Estimation of Vehicle Sideslip Angle Based on Adaptive Extended Kalman Filter,* Shanghai: SAE International.

Gillespie, T. D., 1992. *Fundamentals of Vehicle Dynamics.* 1stt ed. Warrendale: Society of Automotive Engineers Inc.

Global NCAP, 2012-2013. *UN Decade of Action for Road Safety 2011-2020.* [Online]
Available at: http://www.globalncap.org/un-decade-of-action-for-road-safety-2011-2020/
[Accessed 18 January 2014].

Grip, H. F. et al., 2010. Vehicle Sideslip Estimation: Design, implementation, and experimental validation. *IEEE Control Systems Magazine,* 29(5), pp. 36-52.

Hac, A. & Bedner, E., 2007. *Robustness of Side Slip Estimation and Control Algorithms For Vehicle Chassis Control.* Washington, NHTSA.

Hac, A., Nichols, D. & Sygnarowicz, D., 2010. *Estimation of Vehicle Roll Angle and Side Slip For Crash Sensing,* s.l.: SAE International.

Hac, A. & Simpson, M. D., 2000. *Estimation of Vehicle Side Slip Angle and Yaw Rate,* Detroit: SAE.

Harrison, M., 2004. *Vehicle Refinement: Controlling Noise and Vibration in Road Vehicles.* 1st ed. Oxford: Elsevier Butterworth Heinemann.

Hiemer, M., Vitinghoff, A. V., Kiencke, U. & Matsunaga, T., 2005. *Determination of the Vehicle Body Side Slip Angle with Non-Linear Observer Stratergies,* Michigan: SAE International.

Huffaker, R. M., Fuller, C. E. & Lawrence, R. T., 1969. *Application of Laser Doppler Velocity Instrumentation to the Measurement of Jet Turbulance,* s.l.: SAE International.

Johnson, K., Hewett, S., Holt, S. & Miller, J., 2000. *Advanced Physics For You.* 1st Edition ed. Cheltenham: Nelson Thornes.

Kidd, S. et al., 1991. *Speed Over Ground Measurement,* Michigan: SAE International.

Kistler, 2014. *Complete Systems from Kistler for Reliable Measurements of Longitudinal and Transverse Dynamics.* [Online]
Available at: http://www.kistler.com/gb/en/applications/automotive-research-test/vehicle-dynamics-durability/dynamics-testing/products/#correvit-s-350-sensors-cs350a-
[Accessed 14 05 2015].

Koninklijke Philips N.V., 2014. *Phillips Laser Doppler Technology.* [Online]
Available at: http://www.photonics.philips.com/technology/philips-laser-doppler-technology
[Accessed 15 04 2015].

Krantz, W., Neubeck, J. & Wiedemann, J., 2002. *Estimation of Side Slip Angle Using Measured Tire Forces,* Michigan: SAE International.

Lee, S. A. B. H., 2007. *A Study on Optimal Yaw Moment Distribution Control Based on Tire Model,* s.l.: SAE Technical Paper Series.

Lhomme-Desages, D., Grand, C., Amar, F. B. & Guinot, J.-C., 2012. *Doppler Based Ground Speed Sensor Fusion and Slip Control for a Wheeled Rover,* s.l.: Hal Archives.

Liebemann E, F. T., 2007. *More Safety with Vehicle Stability Control ,* s.l.: SAE Papers.

Lin, F. & Zhao, Y., 2007. *A Comparison of Two-Soft Sesning Methods for Estimating Vehicle Side Slip Angle,* California: SAE International.

Measurement Science Enterprise, Inc, 2014. *How an LDV/LDA works.* [Online]
Available at: http://measurementsci.com/how-an-ldv-lda-works/
[Accessed 01 05 2015].

Meng, H., 2014. *Laser Diode Based Self Mixing Sensor For A Vehicle Electronic Stabilty Program,* s.l.: United States Patent.

Milliken, W. & Milliken, D., 1995. *Race Car Vehicle Dynamics.* 1st ed. Warrendale: SAE.

Minghui, L. et al., 2012. *Design of Body Slip Angle Observer for Vehicle Stabilty Control (EMEIT-2012),* Shenyang: Atlantis Press.

Optimum G: Vehicle Dynamics Solutions, 2010. *Sensor Comparison & Evaluation: Vehicle Slip Angle Measurment Methods,* Argentina: s.n.

Oxford University Press, 2014. *Oxford Dictionaries.* [Online]
Available at: http://www.oxforddictionaries.com/definition/english/Coriolis-effect
[Accessed 4 2014].

Pacejka, H. B., 2006. *Tyre and Vehicle Dynamics.* 2nd Edition ed. Oxford: Elsevier : Butterwort-Heinemann.

Piyabongkarn, D., Rajamani, R., Grogg, J. A. & Lew, J. Y., 2009. Development and Experimental Evaluation of a Slip Angle Estimator for Vehicle Stability Control. *IEE Transactions on Control Systems Technology,* January, 17(1), pp. 78-88.

Rajamani, R., 2006. *Vehicle Dynamics and Control.* New York: Springer.

Reppich, A. & Willig, R., 1995. *Yaw Rate Sensor for Vehicle Dynamics Control System,* Detroit: SAE International.

Richardson, N. A., Lanning, R. L., Kopp, K. A. & Carnegie, E. J., 1982. *True Ground Speed Measurement Techniques,* s.l.: SAE International.

Ryu, J., Rossetter, E. J. & Gerdes, C. J., 2002. *Vehicle Sideslip and Roll Parameter Estimation using GPS.* Japan, Stanford University.

Shraim, H., Ouladsine, M. & Annanou, B., 2007. *Robust Virtual Sensors and Controller Design to Improve Vehicle Stability Enhancement in Critcal Situations,* Michigan: SAE International.

Thrun, S. et al., 2006. Stanley: The Robot that Won the Darpa Grand Challenge. *Field of Robotics,* Volume 23, pp. 665-693.

Wolfram Mathworld, 2013. *Control Theory.* [Online]
Available at: http://mathworld.wolfram.com/ControlTheory.html
[Accessed 4 March 2013].

Zanten, A. v., 2000. *Bosch ESP Systems: 5 Years of Experience,* Michigan: SAE Technical Paper Series.

.